

**IMPACT PROPERTIES OF CAST STEEL
SECTIONS WITH SURFACE
DISCONTINUITIES**

**A RESEARCH PROJECT AT CASE INSTITUTE
OF TECHNOLOGY**

**Sponsored by
STEEL FOUNDRY RESEARCH FOUNDATION**

**Charles W. Briggs
Director of Research**

**© by STEEL FOUNDRY RESEARCH FOUNDATION
Rocky River, Ohio September, 1967**

Published and Distributed by Steel Founders' Society of America
Westview Towers, 21010 Center Ridge Road Rocky River, Ohio 44116

TABLE OF CONTENTS

	Page
Scope of the Research Report	3
Summary of the Research Report Conclusions	3
Preface	4
Introduction	6
Selection of Transition Temperature Criteria	8
Effect of Discontinuities on Properties	9
Materials and Procedure	10
Mechanical Properties	13
Surface Discontinuities	15
Gas Cavities	15
Surface Slag Inclusions	18
Hot Tears	20
Welded Cast Steel	23
Metallography	30
Ductile Fracture	33
Brittle Fracture	35
Evaluation of Research	38
Conclusions	40
References	42
Appendix I	43

Steel Foundry Research Foundation

**IMPACT PROPERTIES OF CAST STEEL SECTIONS
WITH SURFACE DISCONTINUITIES**

SCOPE OF THE RESEARCH REPORT

The ability of a steel casting to withstand impact loading without failure is determined by its strength, microstructure, composition, the magnitude of the impact stress, the rate of loading, the ambient temperature, the presence of multiaxial stresses and the presence of stress concentrations.

This investigation utilizes three different types of impact tests with different strain rates and two types of stresses (bending impact and tension impact) to evaluate the effect of different types of surface discontinuities that produce stress concentrations or notches for a cast steel of two different strength levels and microstructures.

The studies of this report are an extension of previous studies of a similar nature as to the determination of surface discontinuities on the static and dynamic (fatigue) properties. These studies were concerned with the determination of surface discontinuities on the dynamic (impact) properties.

SUMMARY OF THE RESEARCH REPORT CONCLUSIONS

The results of tests made on cast steel sections made under dynamic loading in bending impact and tension impact provide significant information concerning the influence of sound sections and sections containing severe surface discontinuities on the impact properties of cast steel.

1. Tempered martensitic structure obtained by quenching and tempering a low alloy (8630) cast steel provided better impact resistance than the ferritic-pearlitic structure obtained by normalizing and tempering. This improvement in toughness was particularly marked in its effect on the transition temperatures obtained with the three types of impact tests (two unnotched types and one notched type).

2. Severe surface discontinuities in cast steel result in increased transition temperatures and diminished fracture energies as compared to cast steel without the discontinuities. Impact ductility and fracture energy in bending are dependent on both the location of the discontinuity and the stress concentration produced by the discontinuity. Location is not a major factor in tension impact.

3. Severe discontinuities in welds made in cast steel showed that the weld discontinuities reduced the impact resistance of the cast steel. The order of decreasing severity was undercut, slag inclusion and incomplete penetration.

4. Brittle fracture energies measured near the ductility transition temperature by impact for casting discontinuities appear related to the stress concentration of the discontinuity (proportional to K_t^{-2}). The K_t values estimated for hot tears are 9 and greater, whereas slag and gas cavity discontinuities were within the range of 1.5 to 2.6.

PREFACE to the RESEARCH REPORT

What constitutes the effect of discontinuities at the surface of a structure on the ability of the structure to perform its intended service? This has not been an easy question for design engineers to answer. Most materials and design engineers have some very strongly held opinions on the importance of discontinuities in structures as revealed by non-destructive testing but actual information on this matter backed with factual data is very limited.

It is a well known fact, however, that surface notches have a pronounced effect on the impact resistance of metals and that surface discontinuities can act as notches. The surface discontinuities employed in the research were gross and very severe ; so severe in fact that they exceed the designated classes of discontinuities as established by ASTM in the non-destructive testing standards ; namely, E 125 Magnetic Particle Reference Photographs and E 71 Reference Radiographs. It was known before testing that these severe surface notches would have an effect on the endurance strength of the cast steel. Likewise the V-notch in the Charpy impact specimen has a pronounced effect on the impact properties of a similar steel test specimen without the machined V-notch.

There seems to be considerable hesitancy by the engineering profession to draw comparisons between the V-notch impact energy and transition temperature with those obtained by testing unnotched test specimens in impact-bending and impact-tension containing severe discontinuities. The differences obtained between the three types of tests are individually concerned with the location of the discontinuities with respect to the maximum stress, the microstructure of the steel at the base of the notch, the severity of the stress concentration on notch acuity and the differences in the dimensions of the three impact specimens. Some of these factors are not well established and any direct comparisons or attempts to draw significant conclusions from a comparison of the three sets of impact test data are not advisable. The only comparisons that can be made are observations concerning the differences between the transition temperature and impact energy of the cast steel specimens without discontinuities and those specimens containing the severe discontinuities. Estimates of what might be the effect of minor or mild types of discontinuities on the impact energy or transition temperature also cannot apparently be made until factual data are available.

Thus, all that can be said is that severe discontinuities do have a pronounced deteriorating effect on the impact energy and change the transition temperature of cast steels. Apparently other studies must be carried on by testing less severe discontinuities or testing entire steel casting with and without discontinuities.

A previous research report by the Foundation issued in August 1966 on The Effects of Surface Discontinuities on the Fatigue Properties of Cast Steel Sections studied discontinuities in bending-fatigue and tension-fatigue test specimens. Such information could be correlated to the notched R.R. Moore test normally employed by design engineers.

It is the desire of the steel casting industry to produce a quality product. However, the higher the degree of quality the more intense the processing requirements and the higher the end product costs. Extra quality beyond normal commercial standards is in most cases not necessary or required because of the lack of information on the importance and value that is placed on the various degrees of discontinuities as observed by non-destructive testing. Severe surface discontinuities are not present in commercial steel castings hence values illustrated by the studies of this report would in all probability not be encountered.

The steel foundry companies through research and the technology which they are generating will continue their progress in the production of quality castings but it may be advisable to point out that unnecessary inspection requirements come high in terms of production costs.

CHARLES W. BRIGGS
Director of Research
Steel Foundry Research Foundation

September 1967

**IMPACT PROPERTIES OF CAST STEEL
SECTIONS WITH SURFACE
DISCONTINUITIES**

**by
E. S. Breznyak and J. F. Wallace
Research Assistant and Professor, Department of Metallurgy
Case Institute of Technology**

**Steel Foundry Research Foundation
in contract with
Case Institute of Technology**

IMPACT PROPERTIES OF CAST STEEL SECTIONS WITH SURFACE DISCONTINUITIES

Introduction

One of the major design problems is the occasion of brittle fracture in steel structures. The most damaging feature is that brittle fractures occur rapidly and without warning. Such failures are not predicted because the nominal stress at time of failure may not be high but exists considerably below conventional design criteria of ultimate tensile strength or of yield strength. Incidence of catastrophic brittle failures from cracks initiating at weld-flaws have been reported for ships and for storage tanks where the material did not appear to develop its normal strength and ductility.(1, 2) The significance of these failures is that simple uniaxial tension testing at slow strain rates and at room temperature may not be the criterion controlling the behavior of a component under stress. This idea is not surprising since the tension test does not reflect the properties of steel parts under situations of constraint, low temperature, high rates of loading, and localized stress concentration generated by the presence of a flaw or a notch, or resulting from structural design.

It is well-known that certain properties of carbon and low alloy steels deteriorate with decreasing temperature. A temperature is defined as the nil ductility temperature (NDT) below which the ability of the steel to absorb energy drops to a very low value.(3) This point shifts to a higher temperature as stress increases and concentrates as in the presence of a notch. Below the NDT point, failure is brittle and is characterized by negligible ductility and occurs by cleavage.

The principal factors which affect the ductile to brittle transition in steel are temperature, rate of load application, stress concentration as in the presence of notch, specimen or part size, material composition and microstructure.

The yield strength of steel increases markedly with a decrease in temperature. Consequently, brittle fracture and failure can occur with a minimum of ductility before yielding. Another phenomenon which appears to be related to the brittle fracture of mild steels is delayed yielding.(4) Steels loaded rapidly to a stress above the yield stress exhibit a time delay before plastic yielding occurs. The time delay increases with decreasing temperature at a constant stress. Since brittle fracture will occur when plastic yielding fails to keep the stress below some critical value, it ap-

pears that a relation should exist between delay yielding and brittle fracture.(5)

The effect of rapid loading on the yield strength of some steels is similar to that of temperature but not as pronounced. However, a relationship exists between lower yield point and strain rate.(5) This increase in strength at higher strain rates may be accompanied by a loss in impact resistance. The ductility transition temperature can be shifted 140 F degrees downward by static loading of Charpy specimens as compared to impact loading.(6) This represents approximately a 30 F degree rise for each tenfold increase in strain rate. The raising of the yield point is shown to be related with the delay time to yield, since yield time increases at a higher strain rate even at normal temperatures.(7) Thus, it is evidenced that the effect of low temperatures, high strain rates, and delayed yield times are interrelated and all promote brittle fracture.

The origin of brittle failures can usually be traced to regions of high stress concentrations which are generated from structural stress concentrations or material discontinuities. The location of these discontinuities are most always external and extend to or originate at the surface of a component. These are produced as the result of the casting process or design and include surface discontinuities of porosity, shrinkage, non-metallic inclusions and design notches of keyways, oil holes, screw threads, sharp angles, rivet holes, weld discontinuities, etc.

The effects of a discontinuity or a notch in a steel section on brittle fracture can be surmised by considering the geometry of a notched impact bar such as a Charpy V notch. As the longitudinal stress at the base of the notch increases, contraction in the thickness direction is constrained by the relatively unstressed material away from the notch and a stress is produced in the thickness direction. This condition results in a state of triaxial stress.(8) The significance of this state is that the longitudinal stress necessary for yielding is increased. Consequently, the fracture strength may be exceeded before plastic yielding can occur and flat, cleavage fracture will result. Finally, the entire flow curve of a notched specimen is raised above that of the unnotched specimen by an amount expressed by a plastic constraint factor. Elastic stress concentration at the base of the notch can be extremely high as notch acuity increases. However, the plastic constraint factor

cannot exceed a value of approximately 3 regardless of how sharp the notch. Thus, it appears that the effects of a notch are to produce a high elastic stress at the notch tip, increase the strain rate, increase the longitudinal stress necessary for yielding, and raise the plastic flow curve. All of these are factors that will enhance the probability for brittle fracture.

The effect of the size of a specimen is generally to increase the temperature at which brittle fracture occurs.(9,10) The toughness of structural grades of steel is influenced by section thickness in two separate ways : metallurgical and geometrical (mass effect). (11) The transition temperature of a given steel usually decreases with increasing section thickness because of the coarser grain size produced by hot working or heat treatment temperatures. This fact indicates that metallurgical structures of thick sections are less tough than thin sections; however, Charpy type impact tests on specimens of varying size but with identical metallurgical structure and geometrically similar notches also show a size effect.(12,13) The geometrical or mass effect explains this phenomenon in terms of stress distribution and stored elastic energy. A thick section offers more constraint to plastic flow than a thin section, particularly in the presence of a notch and therefore, contains a more unfavorable state of stress. The thicker sections also provide a large reservoir for stored elastic energy. The Griffith criteria for brittle fracture require that the elastic strain energy must provide the necessary energy for the formation of the fracture surface and consequently the greater the available stored energy, the greater is the ease with which a rapidly spreading crack can be propagated.(5)

Another important factor controlling the notch toughness of steel is its microstructure.(14, 15,16) An increase of one ASTM grain size of the ferrite phase has been shown to raise the transition temperature by 25 F degrees. The size of the ferrite grains is determined to some extent by the austenite grain size from which they form but it is more strongly influenced by the cooling rate through the transformation range. Nickel and manganese increase the toughness of ferrite, partially by inducing finer grains.(17) Metallographic studies have shown(18) that initial cracking occurs in the ferrite phase at the interface of the ferrite and pearlite or martensite. The explanation put forth is that under applied stress the weaker ferrite is forced to supply the plastic deformation while the stronger dispersed pearlite acts by constraining the ferrite, thereby limiting its flow be-

fore cracking. The transition temperature of a steel is lowered as the microstructure is changed from coarse pearlite through tempered bainite to tempered martensite. Therefore, fully hardened and properly tempered steel results in better notch properties than normalized and tempered steel and considerably better than annealed steel. The high degree of notch toughness of martensite is understandable since the ferrite has an extremely fine grain size with the carbides uniformly dispersed throughout the ferrite.

The studies evaluating the influence of chemical composition of carbon steels on impact strength are sufficiently advanced to permit a qualitative evaluation of the effect of individual elements. The effect of the elements on notch toughness appears to depend on whether the elements are present as substitutional or interstitial atoms in the body centered cubic ferrite lattice.(19) Substitutional solute atoms have a relatively small effect; only nickel, molybdenum and manganese exhibit beneficial effects while chromium, copper, vanadium, and aluminum produce mildly adverse effects.(20) Interstitial elements of carbon, phosphorus, nitrogen, and oxygen all act to reduce notch toughness. For each increase of 0.1 percent carbon, the 15 ft. lbs. transition temperature criterion for Charpy V notch specimens is raised about 25 F degrees ; the 10 ft. lbs. transition is raised about 20 F degrees. Carbon also has a marked effect on maximum energy for fracture; the higher the carbon content, the lower the maximum energy.(20) Phosphorus increases the transition temperature even more rapidly than equal amounts of additional carbon; the 15 ft. lbs. transition temperature is raised about 13 percent for each 0.01 percent increase in phosphorus content.(20) Sulfur, usually present in steels as non-metallic inclusions, reduces ductility and has an adverse effect on impact depending on the type size, amount and distribution present in the alloy.

Welding is another source of discontinuities which can lead to brittle fracture. These discontinuities can be classified as both metallurgical and geometrical. The local application of heat during welding results in changes in the microstructure of the parent material in the heat affected zone usually to the detriment of notch toughness. The geometrical aspect involves stress raising discontinuities represented by cracks, voids, lack of penetration, undercut or slag inclusions in the weld. These discontinuities will have an effect similar to that of a notch, as previously discussed, and will therefore enhance the probability of brittle fracture. Other factors which have been

shown to affect the notch toughness of weldments adversely are residual stresses, entrapped hydrogen, and poor weld design.(21) Poor workmanship is known to have been responsible for catastrophic failures.

Several tests have been devised for measuring the ability of mild steels to resist fracture. These tests such as the V notch Charpy impact, Drop Weight, Tipper, Robertson Crack Arrest, and Lehigh each have a different way of establishing a temperature below which brittle fracture occurs.(21) The width of the transition zone varies with test conditions, the specimen geometry, and the chemical composition of the steel. For a particular steel under consideration, the results of each test cannot necessarily be correlated with the other tests. However, each type of test is effective as a means of comparing the different materials. The most commonly used test is the Charpy V notch and it is recommended that this test always be made in addition to any other desired test for the purposes of comparison.(22)

Selection of Transition Temperature Criteria

Numerous fracture tests have been devised and used to provide information where behavior of materials under conditions of fracture is a problem. These tests may be conducted at a particular temperature of interest such as the minimum service temperature, at room temperature, or over a range of temperatures which will include the entire ductile to brittle transition. Also useful information is obtained from the impact energy required for rupture, ductility measurements, and the fracture appearance of the broken specimen. Confusion can arise in comparing the data from several investigations even when the same test is used if the criterion employed to describe the transition is not uniformly selected. In view of the complexity of this measurement, it is discussed in some detail.

A. Energy Transition

1. Energy at a particular temperature
2. Temperature for a selected impact energy level such as 10 ft. lbs. or 15 ft. lbs.
3. Temperature range for the transition from low energy fracture to maximum energy
4. Maximum energy at 100 percent fibrous fracture appearance

B. Fracture Transition

1. Temperature for which the fracture fibrosity or crystallinity is at some particular level such as 50 or 75 percent crystallinity of the fractured face

C. Ductility Transition

1. For bending loads, lateral contraction measurements at the fracture face at the tension loaded side or lateral expansion at compression loaded side
2. For tension loaded specimens, reduction in area and elongation measurements
3. Temperature at which first indication of ductility is measured. A 1 percent lateral contraction under the notch has been used for Charpy testing.

A typical energy temperature and crystallinity temperature curve showing some of these proposed criteria is given in Figure 1. For the present work three criteria were used to compare the transition behavior of the steel :

- A. Ductility Transition Temperature (DTT)- defined as the temperature below which no plastic deformation was detected as determined by lateral contraction measurements for the bending tests and by percent reduction of area and percent elongation for the tension tests.
- B. 50 percent Fibrous Transition Temperature (.5FTT)-defined as that temperature at which the fracture face appearance was 50 percent fibrous and 50 percent crystalline.

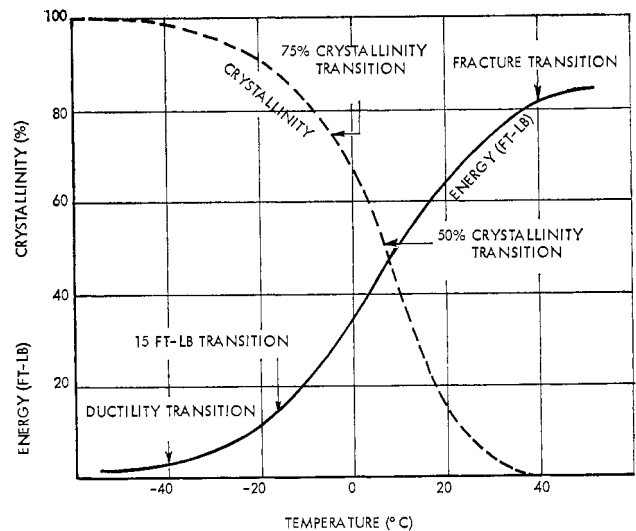


Figure 1—Typical energy - temperature and crystallinity - temperature curve showing proposed criteria for assessment of steels.

C. Complete Fibrous Transition Temperature (CFTT)-defined as that temperature at which the fracture face was essentially completely fibrous (90 to 100 percent). This point coincided with the maximum energy absorption at the upper range of the transition.

Microstructural Examination . . . Knowledge of the microstructure in the regions near the discontinuities is helpful in determining transition temperatures. The microstructure, by using standard light microscopy techniques in discontinuity areas, is compared to that of the basic material to determine the extent of any structural differences.

Electron fractography techniques also are helpful and used to study fracture morphology in the brittle, ductile and intermediate fracture regions. A two-step replicating technique was used in the studies of this report. The subsequent viewing and photography of the replicated surfaces were performed using a Philips Electron Microscope Model EM 100-B.

Effect of Discontinuities on Properties

A minimum of information is available which definitely analyzes the effects of discontinuities on the dynamic properties of various steels. The bulk of information available, concerned with impact loading, is performed with specimens containing carefully machined notches. Most of the available information on the effects of discontinuities has been obtained by slow room temperature tension and bend tests. For example, a study of the effect of mass on the properties of 4330 cast steel having 6-inch-square and 8-inch-round sections showed that both tensile strength and ductility were reduced away from the ingot surface.(23) The loss in properties was attributed to mass effect caused by the increased amount and greater intensity of the alloy segregation and larger dendritic arm spacing and greater concentrations of non-metallic inclusions toward the center of the castings.

In a similar effort(24) the mass effect on the tensile and Charpy V notch properties of four heats of various low alloy cast steels was investigated. At the centers of the castings where segregated inter-dendritic areas and agglomerations of inclusions are prevalent, slight reductions were found in tensile and yield strength while tensile ductility was noted to be greatly affected. However, Charpy V notch impact values measured in various locations in the castings were found to be only slightly

affected. These results were surprising in view of the limited tensile ductilities observed for the more slowly solidified section centers.

Another investigation(25) was initiated to establish a correlation between mechanical properties and imperfection size as determined by radiographic standards. Solidification imperfections of both porosity and shrinkage types with 4140 cast steel heat treated to a strength level of 180,000 to 200,000 psi were studied. A least squares statistical regression analysis showed a linear decrease in tensile strength with imperfection size increases. No marked differences between the two types of imperfections in reducing the tensile strength was observed.

In similar investigations,(26, 27) attempts were made to correlate solidification imperfections with tensile properties of cast stainless steel CA-15 (12 Cr) plates. Radiographic techniques were used to rate the porosity solidification imperfections on 0.1, 0.2, 0.3, and 0.6 inch thick plates heat treated to 180,000 to 200,000 psi ultimate strength. Results indicated that as the intensity or size of the imperfection increased, the tensile strength and elongation decreased significantly. The yield strength showed no marked change with increasing intensity or size of imperfection for the range investigated. It should be pointed out that the discontinuities were so prominent that they affected materially the cross section of the test specimen.

Another investigation on the effect of centerline and gross shrinkage porosity on 8630 cast steel(28) showed that severe centerline shrinkage porosity (Class 6 ASTM E-71) resulted in less than a 10 percent reduction in tensile strength ; however, gross cavity shrinkage produced strength losses of up to 50 percent.

Some investigations have been carried out to find the effects of porosity on the mechanical properties of welds. In one study(29) in the specimen cross section of mild steel (35,000 psi yield strength) welds were reduced by porosity up to 7 percent without significantly changing the mechanical properties as determined by room temperature static tensile and Charpy V notch impact tests. The shape and distribution of the porosity did not cause significant differences in any of the tests. A similar study(30) was conducted to evaluate porosity effects in a higher strength steel weld (100,000 psi yield strength), The experimental results showed that the cross section of welds could be reduced up to 5 percent without appreciably changing the mechanical

properties measured. The effect of shape, location and distribution appeared negligible in the room temperature tensile and Charpy V notch impact tests. In bend tests, the porosity effects were found to be more critical if located near the convex surface. Above 5 percent weld porosity, all mechanical properties were noted to fall away sharply to low levels.

From these data it was evident that a need existed for information relative to the effect of casting and weldment discontinuities on the dynamic properties of steel structures. Comprehensive answers are needed to the following questions : What types and amounts of discontinuities can be contained in an economical and reliable design ? If a discontinuity is present, should the part be accepted, reworked or rejected? If the engineer is to accept a part containing discontinuities, he will need quantitative data as a basis for evaluating the effects of these discontinuities. If the part containing the discontinuity can be accepted, therefore it was produced more economically than if it required reworking or had been rejected. Most important, if the basis for evaluation is feasible, the part's reliability in service is assured.

A two-part investigation was undertaken to study the effects of discontinuities on the properties of steel castings under dynamic loading. The first part evaluated effects of cast steel sections under fatigue loading of reverse torsion and reverse bending and the results have been reported.(31) Part two of this investigation as reported herein is concerned with adding to the knowledge of impact behavior of cast steel and cast steel weldments containing various surface discontinuities. For this study a popular Ni-Cr-Mo cast steel (8630) was selected. The specific discontinuities investigated in the designated cast material were surface discontinuities ; slag inclusions, hot tears and gas cavities. Welds were produced in the cast steel ; the impact behavior of sound welds in the cast steel were compared to welds with undercut, internal slag inclusions and incomplete penetration. Sound stock was cast to provide test specimens for the purpose of control and comparison. Room temperature tensile data were obtained for randomly selected heats. Two primary heat treatments were employed ; quench and temper to a 130,000 psi to 150,000 psi level and normalized and temper to a 80,000 to 90,000 psi strength level. A few studies were also conducted with quench and temper and normalize and temper steel specimens heat treated to the same 110,000 to 120,000 psi tensile strength level.

Materials and Procedure

General Casting Practice . . . The steel produced for this investigation was a cast Ni-Cr-Mo (8630) composition. Conventional basic induction melting practice and aluminum deoxidation were used to produce the test castings. Nine different heats of steel were employed. The complete compositions of these heats appear in subsequent tables of impact data in Appendix I. In general, the percentage composition ranges were :

C	Mn	Si	Cu
0.28-0.33	0.64-0.90	0.19-0.38	0.40-0.60
Mo	P	S	Acid Soluble Al
0.19-0.25	0.014-0.030	0.013-0.032	0.044-0.070

The steel was cast into sand molds to produce bars for tensile impact specimens and plates for bend impact specimens. Tensile specimens and Charpy V notch specimens were machined from these sections.

Production of Bending and Tensile Impact Specimens . . . The casting discontinuities investigated included hot tears, slag inclusions and gas cavities. The procedures used for incorporating these flaws into the castings have been thoroughly detailed in the Steel Foundry Research Foundation's Research Report published in August 1966.(31) Briefly, hot tears were obtained by hindered contraction and formed perpendicularly to the longitudinal axis of the bars and plates. Large surface slag inclusions were produced by embedding slag particles into the drag surface of the mold cavity Gas cavities were obtained in the bend specimens by eliminating the aluminum as the final deoxidizer and using only ferrosilicon. The size and distribution of the gas cavities produced varied, therefore an alternate method was employed for the tension impact specimen. A single hole 1/16 inch in diameter was drilled normal to the longitudinal axis at the gage center of the (0.357 inch diameter) tension impact specimens. The severities of the hot tears, slag inclusions and gas cavities were rated according to ASTM reference radiographs E71-64 and ASTM magnetic particle reference photographs E125-63.

Three severities of shrinkage were produced by improper risering techniques in the bending impact specimens. However, only two severities could be successfully established within the smaller gage section of the tension impact spec-

imens. The severities of the shrinkage discontinuities were determined by ASTM reference radiographs E71-64 and ASTM magnetic particle reference photographs E125-63.

Bending and tension impact specimens free of discontinuities were also produced for control and comparison purposes ; also, tensile and Charpy V notch specimens were machined from coupons to establish the base mechanical and impact properties of each heat.

Welding Procedure . . . The bending and tension impact specimens were welded by a commercial welding company. The types of weld discontinuities investigated were : 1) sound weld, 2) sound weld with the reinforcing head removed by machining, 3) weld undercut after machining, 4) weld slag inclusions after machining, and 5) weld incomplete penetration after machining.

The low hydrogen welding electrodes used were Hobart LH 918M to obtain notching mechanical properties after heat treatment. A pre-heat temperature of 300 degrees F was employed and a post heat temperature of 1100 degrees F for one hour was applied to the specimens immediately after welding to retard cooling and prevent the formation of underbead cracks.

A symmetrical, double vee butt joint was employed and is shown with the order of welding passes in Figure 2a. The tension impact specimen weld joint design is shown in Figure 2b and the machined specimen is shown in 2c. A 0.045 inch diameter welding electrode of designation National Standard 2 1/4 Cr, 1 Mo was selected to prevent specimen overheating and to permit multiple weld passes in the small weld section. The weld material composition was similar to the LH9018 electrode used for the bending specimens. The weld metal was deposited using Heliarc tungsten inert gas technique (TIG) . Since the smaller weld rod was not coated, an argon cover (a number 8 cup with a flow rate of 12 cubic ft./hr.) was used during the welding.

Machining . . . The bending impact specimens were machined to the test bar dimensions of 7 1/2 inches long by 1 inch wide by 1/2 inch thick from as-cast plates 8 inches long by 1 1/4 inches wide by 5/8 inch thick. The plates were ground on a rotary vertical spindle : a Blanchard surface grinder using a selective grinding procedure to assure equal stock removal from opposite surfaces. This technique was closely monitored when grinding the bars containing shrinkage in order to maintain the shrinkage centrally with respect to

the surfaces of the finished machined bar. Slow table and spindle speeds of 9 and 900 rpm, respectively, with a minimal automatic feed of 0.004 inch per minute were used. These slow speeds and feeds were used in conjunction with a resinoid bonded, cool cutting wheel to minimize generation of heat and residual tensile stresses in the bending specimens.

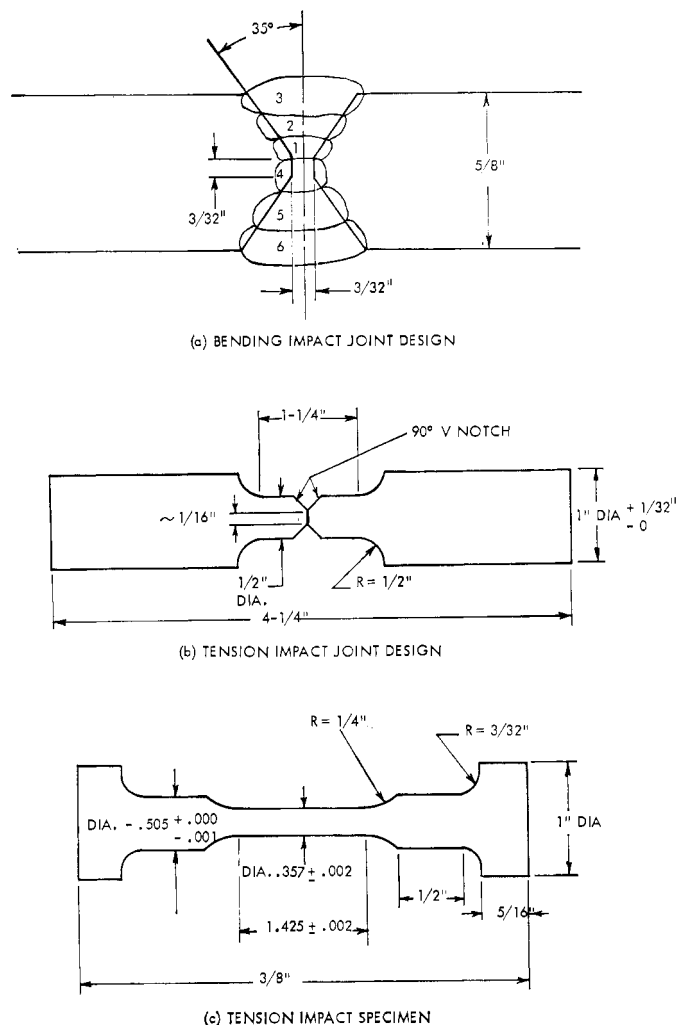


Figure 2—Symmetric of joint design (not to scale).

The tension impact specimens were made by initial rough turning and finished by contoured wheel grinding. The finished machined dimensions of the tension impact specimens are shown in Figure 2c. Charpy V notch specimens were made to dimensions according to ASTM specification. The 0.010 inch radius at the base of the 45 degree included angle V notch was lapped to remove marks of machining. The tensile specimens used to determine the static strengths of the various heats had a diameter of 0.357 inch and a gage length of 1.40 inches.

Heat Treatment.. . The tensile strength levels selected were 80,000 to 90,000 psi and 120,000 to 145,000 psi with some limited number of specimens at 110,000 to 120,000 psi tensile strength. These levels were obtained by two heat treatments: (1) normalize and temper and (2) water quench and temper. Specimens were water quenched from the tempering temperature. The specimens tested with the weld bead in place were heat treated under a protective neutral atmosphere to avoid decarburization. The other weld specimens were heat treated in gas fired furnaces. All the other specimens containing gas cavities, hot tears, surface slag inclusions and quench cracks were austenitized in salt pots prior to quenching ; the tempering was conducted in electric resistance heated furnaces.

Mechanical Tests.. . The machined specimens were subject to various mechanical tests which included standard tensile, impact Charpy V notch, impact tensile and impact bend testing. Tensile testing was performed as a control to ascertain the static strength and ductility response of the steel to the thermal treatments. The data obtained with the Charpy V notch testing served as a control and provided a baseline for comparison with results of the impact testing with the scaled up bending specimens and with the tension impact testing. The Charpy testing was performed on a Widermann-Baldwin Pendulum Type Impact

Tester with a 240 ft. lb. capacity and a pendulum velocity at impact of 204 in./sec.

Bend testing of the scaled up specimens was completed at Watertown Arsenal, Watertown, Massachusetts, on one of the three largest pendulum impact machines in the world. The 2200 ft. lb. energy capability of this testing apparatus allowed for a scale up of the bending specimens to dimensions as previously described. The arm length is 80 inches and swings through an angle of 161 degrees as measured from the rest position. The velocity generated at the pendulum striker anvil just prior to impact is 346 in./sec. The span length of the specimen holding fixtures was 4 7/8 inches. Those bending specimens (specimen length equals 7.5 inches) which did not fracture were required to bend through an angle of 112 degrees to clear the holding fixture span.

A technique for tension impact testing was developed to measure and record drop weight velocities prior to and after fracture. From these data, the energies required to affect specimen fracture were calculated. The system which was used, shown in Figures 3a and 3b, consists of a Phillips tube counter, a chronograph adapter gating circuit, and silicon photovoltaic light sensors. Two light sources and the light sensors are housed in opposite legs of a specially constructed horse-shoe shaped bracket mounted to the right of the impact fixture shown in Figure 2b. A light sensor

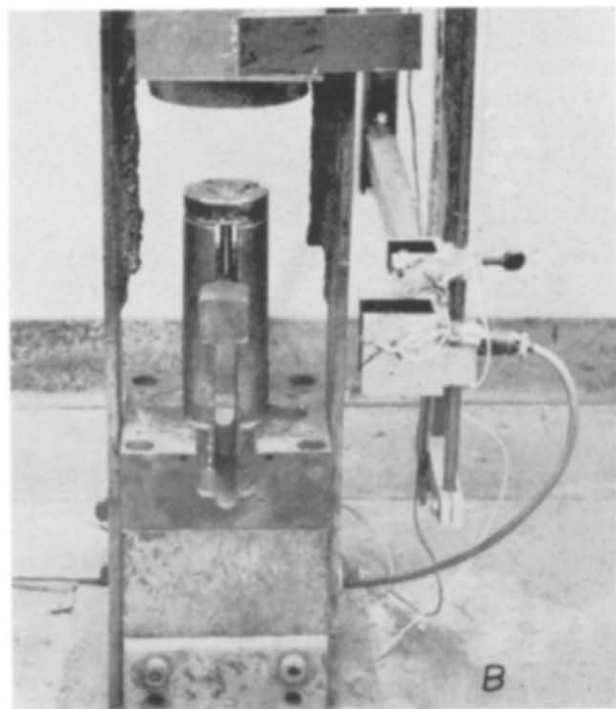
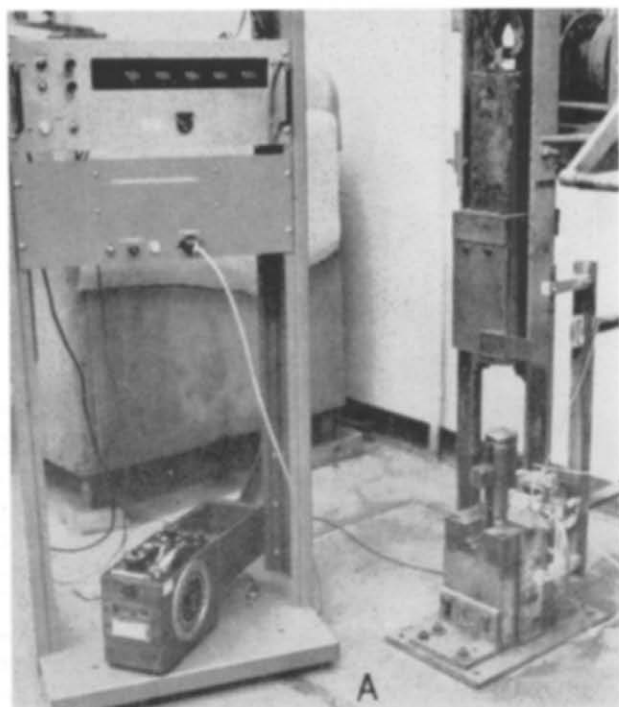


Figure 3—(a) Holding fixtures and recording instrumentation for tension impact test apparatus and (b) close up of holding fixtures and light sensor brackets.

is located behind each of two slits which were milled 0.020 inch wide by 1/2 inch long at exactly one inch separation. As the 80-pound drop weight descends from a fixed height of 10.5 feet, a protruding shield passes over the first slit, blocking the incident light on the sensor. The sensor then sends a signal to the gating circuit which acts as a high speed electronic switch and activates the counter. The counter records counts at a rate of 100,000 counts per second until the shield passes over the second slit, at which time the signal from the second light sensor to the gating circuit stops the counter.

The number of total counts for the drop weight to traverse one inch is recorded on the tube counter and thus the velocity is computed. The upper light sensor was positioned 3/4 inch below the initial drop weight contact with the lower specimen crossbar holding fixture in order to record the drop weight velocity (v_f) after specimen fracture. The initial velocity (v_o) was determined by unobstructed free fall and was recorded at 26 ft./sec. (312 in./sec.) at the position of impact. This free fall velocity (v_o) was exactly that calculated from the known height (h) of the drop [$v_o = (2gh)^{1/2}$], indicating a negligible friction loss from the drop weight guide rails. From a knowledge of the initial velocity (v_o) and the final velocity (v_f) and the mass of the drop weight (m_1) and the mass of the lower crossbar specimen holder (m_2), the energy (E) for fracture was computed as follows:

$$E = \frac{1}{2}m_1 v_o^2 - \frac{1}{2}(m_1 + m_2) v_f^2$$

The degree of uncertainty with this system is 10 microseconds while the time duration for fracture was in the order of 1 millisecond, well within recording capability of this system. From the energy relation above, it is implied that no energy losses in the system, such as heat, occur and that the final velocity of the specimen crossbar holder is the same as that of the drop weight. This latter assumption was also investigated by high speed photography. From the high speed photographs a comparison was made with the counter technique of the drop weight velocities after fracture.

Comparison of the velocities computed from the counter readings to those taken from the photography data shows the former to be higher in all cases. However, the maximum deviation from the high speed photography data was less than 5 percent for these tests, indicating a high degree of correlation between the two testing techniques. A third method was used to compare fracture energies with those obtained using the counter technique. Strain gages were mounted on the

lower impact holding fixture to provide force-time oscilloscope traces. The force-time curves were converted to force-elongation curves. The area under the force-elongation curves provided the fracture energy values for comparison with the other techniques used. In all three cases higher impact values were recorded for the counter technique than for the converted force-time traces. The maximum deviation from the counter technique is 9.0 percent which is considered to be good in view of the arbitrary method used in tracing the best mean curve through the vibrational fluctuation of the force-time trace and the approximations used in the subsequent conversions and calculations.

Mechanical Properties

The strength levels and ductilities for the various heats as measured by the standard room temperature tensile testing are reported in Table 1. The heats are also identified in terms of heat treatment, types of impact tests and discontinuities. The reported hardness values shown in Table 1 are an average of at least six readings from three impact specimens from each heat. The Brinell hardness numbers when converted to approximate ultimate tensile strength levels are comparable to the values obtained for the tension tested keel block stock.

Charpy V notch impact values plotted in the form of ductile to brittle transition curves are shown in Figure 4 for three heats of quenched and tempered, and normalized and tempered materials. These are heats that were selected randomly to provide a control test or a baseline for comparison with subsequent impact testing. The impact energy data for fibrous fracture condition and lateral expansion of these steels are listed in the tables in Appendix I. It will be observed from Figure 4 that the transition occurs more

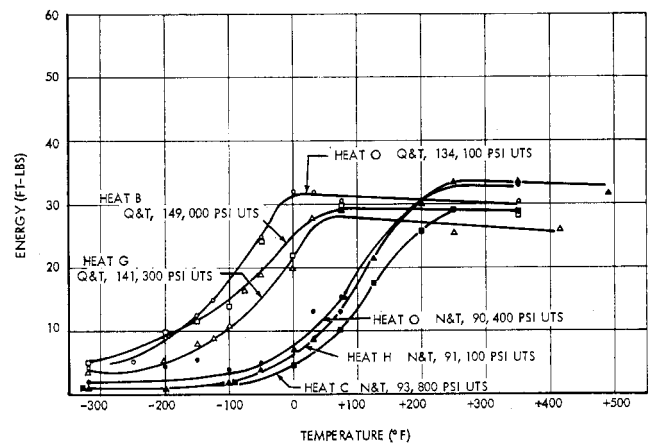


Figure 4—Charpy V-notch test results for three randomly selected heats as indicated.

TABLE 1
Mechanical Property Data for Steel Specimens

Heat No.	Heat Treatment	Specimen Number	Tensile Strength 1000 psi	0.2% Y.S. 1000 psi	Red. of Area %	Elong. in 1.4 in. %	Brinell Hardness Number	Impact Specimens	Discontinuity
A	Quench & Temper	1	131.6	121.6	45.9	16.8	285	Bending	Sound
		2	132.4	122.0	39.1	15.7	284		
		Avg.	132.0	121.8	42.5	16.3	285		
A	Norm. & Temper	1	87.5	58.8	31.5	20.2	169	Bending	Sound
		2	88.4	59.0	34.6	21.0	171		
		Avg.	88.0	58.8	33.1	20.6	170		
B	Quench & Temper	1	148.3	141.0	28.0	13.5	322	a) Charpy V b) Tension c) Tension	Sound Sound & Cavity As-Weld
		2	150.2	141.2	23.5	12.9	316		
		Avg.	149.3	141.1	25.6	13.2	319		
C	Norm. & Temper	1	93.8	59.5	30.3	22.0	156	a) Charpy V b) Tension c) Tension	Sound Sound & Cavity As-Weld
		2	93.8	59.7	33.5	24.1	149		
		Avg.	93.8	59.6	31.9	23.1	153		
D-1	Quench & Temper	1	111.3	93.7	44.1	21.4	238	Charpy V	Sound
		2	109.6	91.5	34.4	17.2	237		
		Avg.	111.0	92.6	39.3	19.3	238		
D-2	Norm. & Temper	1	121.6	100.0	11.9	10.7	250	Charpy V	Sound
		2	116.7	97.4	11.9	8.9	248		
		Avg.	119.2	98.7	11.9	9.8	249		
G	Quench & Temper	1	142.0	132.0	26.5	12.1	300	Charpy V	Sound
		2	140.6	130.4	27.5	13.6	296		
		Avg.	141.3	131.2	27.0	12.9	298		
H	Norm. & Temper	1	91.3	57.0	32.0	23.5	187	Charpy V	Sound
		2	90.8	55.5	34.0	25.0	183		
		Avg.	91.1	56.3	33.0	24.3	185		
J	Quench & Temper	1	137.0	125.2	32.6	16.6	286	Bending	Gas Cavities
		2	135.4	124.0	33.4	15.8	290		
		Avg.	136.2	124.6	33.0	16.2	288		
J	Norm. & Temper	1	82.1	50.4	38.0	25.1	163	Bending	Gas Cavities
		2	83.2	51.0	36.2	24.8	156		
		Avg.	82.7	50.7	37.1	25.0	160		
K	Quench & Temper	1	132.2	123.2	34.5	15.0	286	Bending	Surface Slag
		2	129.2	119.8	35.3	14.8	284		
		Avg.	131.2	121.5	34.9	14.9	285		
K	Norm. & Temper	1	89.8	61.7	43.6	22.1	186	Bending	Surface Slag
		2	90.8	61.8	40.0	20.0	184		
		Avg.	90.3	61.8	41.8	21.1	185		
L	Quench & Temper	1	131.2	122.4	33.2	15.1	267	Bending	Hot Tear
		2	132.0	123.2	30.6	15.0	273		
		Avg.	131.6	122.8	31.9	15.1	270		
L	Norm. & Temper	1	86.4	50.7	38.2	21.6	172	Bending	Hot Tear
		2	84.8	51.0	36.2	20.2	170		
		Avg.	85.6	50.9	37.2	20.9	171		
M	Quench & Temper	1	136.6	127.4	29.4	12.9	290	Tension	Surface Slag
		2	136.4	127.4	26.4	13.5	288		
		Avg.	136.5	127.4	27.9	13.2	289		
M	Norm. & Temper	1	84.4	54.0	27.9	23.2	167	Tension	Surface Slag
		2	84.4	54.8	30.7	25.0	168		
		Avg.	84.4	54.4	29.3	24.1	168		
N	Quench & Temper	1	128.3	118.5	36.3	15.0	278	Tension	Hot Tear
		2	130.0	119.9	37.1	15.0	276		
		Avg.	129.2	119.2	36.7	15.0	277		

TABLE 1—(Continued)

Heat No.	Heat Treatment	Specimen Number	Tensile Strength 1000 psi	0.2% Y.S. 1000 psi	Red. of Area %	Elong. in 1.4 in. %	Brinell Hardness Number	Impact Specimens	Discontinuity
N	Norm. & Temper	1	91.3	58.0	34.0	25.0	179	Tension	Hot Tear
		2	89.7	56.3	35.2	26.3	178		
		Avg.	90.5	57.4	34.6	25.7	179		
O	Quench & Temper	1	134.1	118.9	32.7	14.2	262	a) Charpy V b) Bending	a) Sound b) As-Weld
		2	134.0	120.8	34.4	15.3	265		
		Avg.	134.1	119.9	33.6	14.8	264		
O	Norm. & Temper	1	89.7	62.3	33.2	20.4	186	a) Charpy V b) Bending	a) Sound b) As-Weld
		2	91.0	62.9	33.5	22.9	188		
		Avg.	90.4	62.6	33.4	21.7	187		

sharply and at lower temperatures for the quenched and tempered heat treated cast steels compared to the normalized and tempered cast steels. Above the completely fibrous transition temperature, the fracture energy for both microstructures are at about the same level in spite of the differences in strength.

Figure 5 shows the ductile to brittle transition curves for two cast steels of relatively the same strength level. One of the steels has been quenched and tempered and the other has been normalized and tempered. It can be seen that the quenched and tempered steel gives the best impact properties. The impact energy data for fibrous fracture condition and lateral expansion of these steels are listed in the tables in Appendix I.

The reproducibility of the data is indicated in Table 2 where the transition temperature data are summarized for the Ni-Cr-Mo cast steels. The ductility transition temperature of -200 degrees F for the quenched and tempered materials is shown to be 100 F degrees below that observed for the normalized and tempered. When the 50 percent fibrous (.5FTT) and completely fibrous transition temperature (CFTT) are compared for each of the two property levels, a greater divergence is noted, that is, approximately 125 F degrees and 170 F degrees, respectively. The scatter observed in the impact levels within each structure condition are normally expected and can be attributed in part to variations during experimentation and to slight variations in the strength levels of the steels.

Surface Discontinuities

Impact energy-temperature transition curves for the surface discontinuities of gas cavity, slag inclusions, hot tear and welding discontinuities have been constructed from the test data. In each case the various discontinuities are compared to

sound steel test specimen data. Ductility, fibrosity and impact energy data are listed for the test temperature range and the values are listed in the tables in Appendix I. The degree of severity of the various discontinuities rated according to ASTM specifications are shown in Table 3. The transition data are summarized in Tables 4 and 5.

Gas Cavities

Gas cavity discontinuities appear as surface defects but can extend in depth into the castings. The appearance of gas cavities at the surface and in the fractured sections are shown with bending impact energy-temperature curves in Figure 6. Although the gas cavity size and distribution varied to a slight degree among the cast bars, the



Figure 5—Charpy V-notch test results for quenched and tempered and normalized and tempered steels of the same strength level.

TABLE 2
Impact Transition Data for Charpy V Notch Specimens
Ni - Cr - Mo (8630) Cast Steel

Heat No.	Condition	First Indication of Ductility		50% Fibrosity* Transition		90-100% Fibrosity* Transition	
		(Ft. Lbs.)	Temp. (°F)	(Ft. Lbs.)	Temp. (°F)	(Ft. Lbs.)	Temp. (°F)
B	Quench & Temper 149,000 PSI UTS	10.0	-200	24.0	-50	29.0	+50
G	Quench & Temper 141,300 PSI UTS	5.0	-200	19.0	-50	28.0	+32
O	Quench & Temper 134,100 PSI UTS	9.0	-200	25.0	-50	32.0	+32
D-1	Quench & Temper 111,000 PSI UTS	5.0	-200	20.0	-125	40.0	0
D-2	Norm. & Temper 119,200 PSI UTS	4.0	-100	19.0	+115	35.5	+200
C	Norm. & Temper 93,800 PSI UTS	3.0	-100	12.5	+75	28.0	+225
H	Norm. & Temper 91,100 PSI UTS	2.0	-100	15.5	+75	30.0	+200
O	Norm. & Temper 90,400 PSI UTS	5.5	-150	15.5	+75	30.0	+200

*See procedure for discussion of criteria for transition temperature determination.

TABLE 3
ASTM Classification of Discontinuities in Impact Specimens

Type of Impact Specimen	Discontinuity	(ASTM) Severity Classification	Unacceptable for Steel Castings or Welds
Tensile	Cavity	V-2 (E125) A-6 (E71-64)	For all classes 1 through 5
Bending	Gas Cavity	V-2 (E125) A-6 (E71)	For all classes 1 through 5
Tensile & Bending	Surface Slag Inclusions	III-5 (E125) B-6 (E71)	For all classes 1 through 5
Tensile & Bending	Hot Tears	I-5 (E125) D-6 (E71)	For all classes 1 through 5
Tensile	Weld-Incomplete Penetration	VI-2 (E125) 5-C (E99)	For all classes A through D
Bending	Weld-Incomplete Penetration	VI-2 (E125) 5-D (E99)	For all classes A through D
Tensile & Bending	Weld-Undercut	VI-3 (E125) 9-E (E99)	For all classes A through D
Tensile & Bending	Weld-Slag Inclusions	VI-4 (E125) 3-D (E99)	For all classes A through C

data are reasonably consistent. The area occupied by the gas cavity discontinuities ranged from 12 to 21 percent. The severity of the transition shift to higher temperatures of cavity containing bars as compared to sound bars was second only to the hot tears. The CFTT was increased by 100 F

degrees over the sound materials for both structure conditions. Above the CFTT the fracture energy diminished to approximately 25 percent of the sound material for the quenched and tempered and 35 percent for the normalized and tempered bars, respectively.

TABLE 4
Impact Transition Data For Selected Criteria
Casting Discontinuities

Heat No.	Condition	Type of Test	Discontinuity	First Indication of Ductility		50% Fibrosity Transition		90-100% Fibrosity Transition	
				(Ft.-Lbs.)	Temp. (°F)	(Ft.-Lbs.)	Temp. (°F)	(Ft.-Lbs.)	Temp. (°F)
K	Q&T	Bending	Surface Slag	134	-200	200	-150	380	-75
M	Q&T	Tension	Surface Slag	70	-250	90	-140	115	-70
K	N&T	Bending	Surface Slag	85	-150	320	-35	480	0
M	N&T	Tension	Surface Slag	40	-200	105	-50	160	0
L	Q&T	Bending	Hot Tears	78	-150	—	—	106-380	+50
N	Q&T	Tension	Hot Tears	78	<-110	70	-110	90	+50
L	N&T	Bending	Hot Tears	64	-40	—	—	164-377	+200
N	N&T	Tension	Hot Tears	25	-110	40	0	95	+200
J	Q&T	Bending	Cavities	80	-175	120	-150	190	-40
B	Q&T	Tension	Cavities	73	-250	80	-125	90	-50
J	N&T	Bending	Cavities	80	-150	230	+10	360	+75
C	N&T	Tension	Cavities	75	-150	115	-50	125	+75

TABLE 5
Impact Transition Data For Selected Criteria
Welding Discontinuities

Heat No.	Condition	Type of Test	Discontinuity	First Indication of Ductility		50% Fibrosity Transition		90-100% Fibrosity Transition	
				(Ft.-Lbs.)	Temp. (°F)	(Ft.-Lbs.)	Temp. (°F)	(Ft.-Lbs.)	Temp. (°F)
O	Q&T	Bending	Sound as	79	~-321	60	~-290	1220-1500	-200
B	Q&T	Tension	Machined	80	-250	80	-250	300	-200
O	N&T	Bending	Sound as	106	-200	730	-150	1300	-100
C	N&T	Tension	Machined	126	-200	125	-200	380	-110
O	Q&T	Bending	Sound as Welded	—	<-250	400	-290	950-1200	-200
B	Q&T	Tension	Sound as Welded	~60	-250	60	-250	260	-175
O	N&T	Bending	Sound as Welded	120	-200	550	-130	1250	-100
C	N&T	Tension	Sound as Welded	75	-200	110	-175	280	-100
O	Q&T	Bending	Slag Porosity	70	-200	210	-125	560	-75
B	Q&T	Tension	Slag Porosity	40	-150	60	-110	95	-50
O	N&T	Bending	Slag Porosity	100	-200	500	-50	730	-25
C	N&T	Tension	Slag Porosity	40	-110	90	-25	150	0
O	Q&T	Bending	Undercut	35	-200	150	-125	500	-75
B	Q&T	Tension	Undercut	80	-200	120	-175	200	-150
O	N&T	Bending	Undercut	230	-125	350	-75	550	-25
C	N&T	Tension	Undercut	70	-150	135	-125	230	-110
O	Q&T	Bending	Incomplete Penetration	100	-250	250	-200	630	-150
B	Q&T	Tension	Incomplete Penetration	50	-200	100	-175	220	-150
O	N&T	Bending	Incomplete Penetration	220	<-150	470	-125	800	-60
C	N&T	Tension	Incomplete Penetration	50	-150	100	-125	250	-110

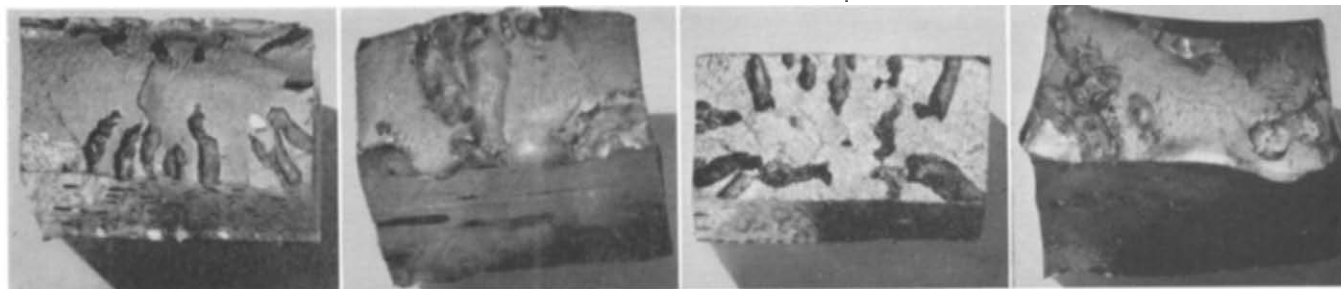
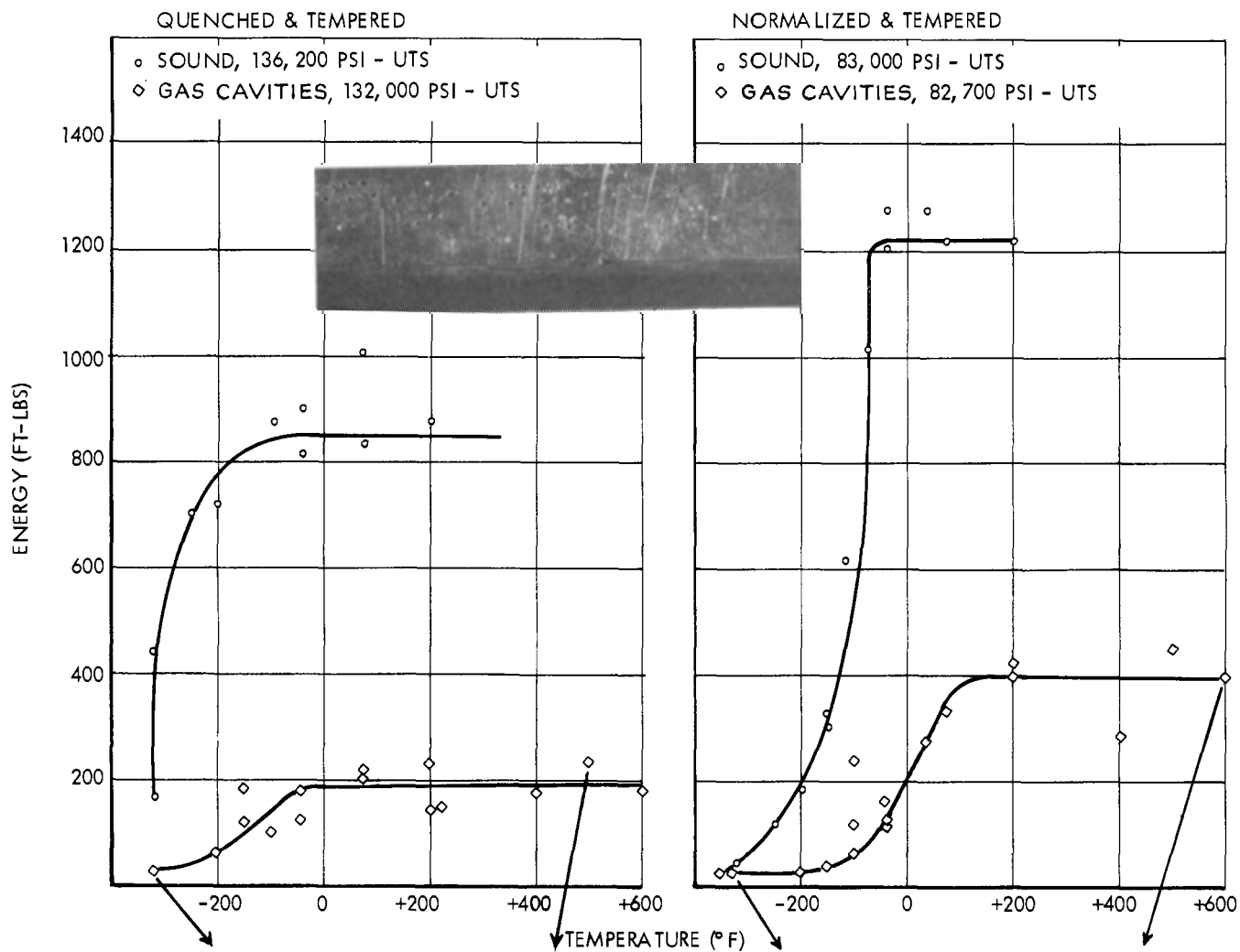


Figure 6—Bending impact test results with gas cavity discontinuities.

The tension impact energies observed with the gas cavity discontinuities also were affected. Because of the small gage section of the tension bars, cavities could not be produced during the casting process with sufficient reproducibility and therefore were simulated by drilling a 1/16-inch diameter hole in the test bars prior to heat treatment. The cavity produced occupied an area of 23 percent of the gage section; this constitutes a pronounced portion of the cross section. A photograph of the resulting cavity in the tension bar and the fracture surfaces obtained are shown

with the fracture energy curves in Figure 7. The transition temperatures are comparable to those obtained with the bending impact tests. The fracture energies above CFTT were also markedly reduced to approximately 25 to 30 percent of that of sound cast steel for both structure conditions.

Surface Slag Inclusions

The slag inclusions of the surface discontinuities least affected the transition temperatures in the bending tests as compared to sound material. The appearance of surface slag and representative

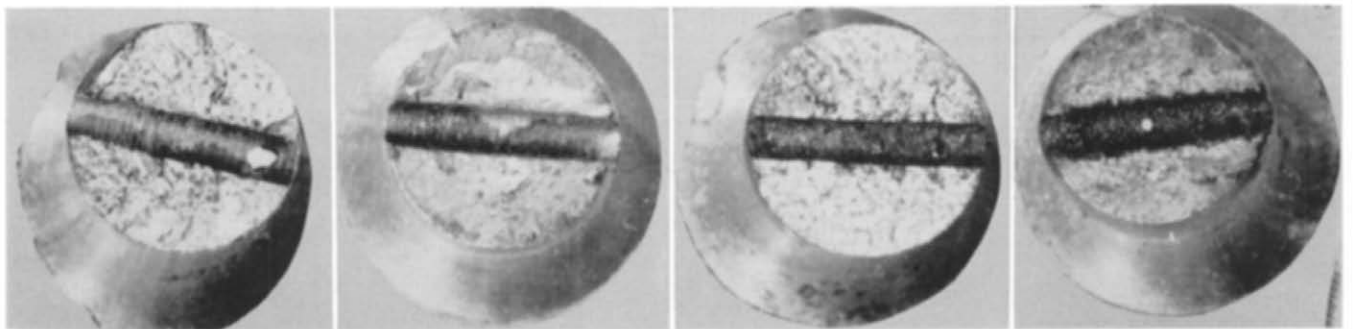
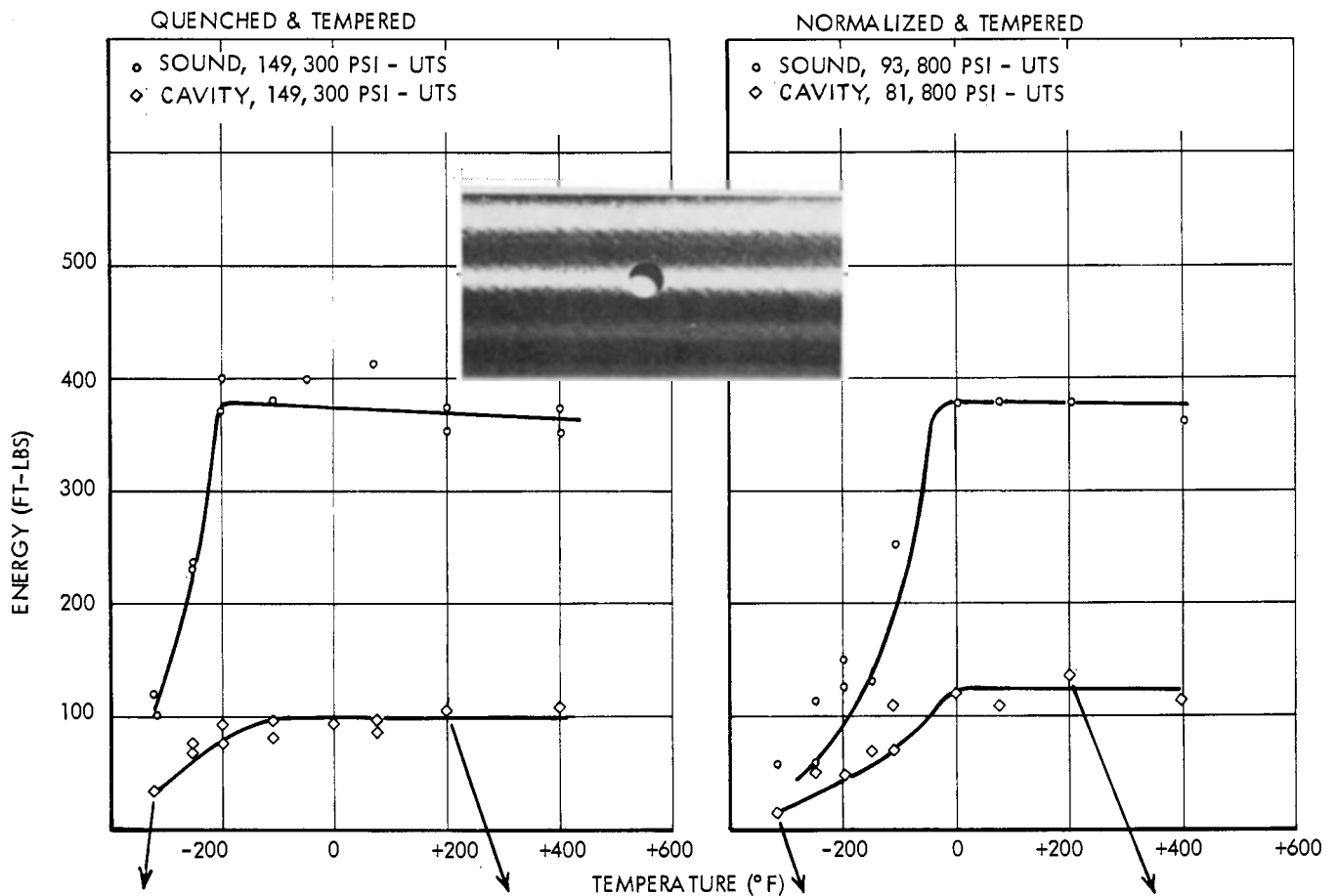


Figure 7—Tension impact test results with gas cavity discontinuities.

examples of the fracture faces are shown with the impact energy curve for the bending tests in Figure 8. The total areas of the slag projected into the cross section of the bending specimens were less than 5 percent. The fracture energy above the CFTT as compared to sound material was diminished to approximately 50 percent for the quenched and tempered and 40 percent for the normalized and tempered bars, respectively. The transition data for tension impact bars containing slag were similar to those obtained with the bending tests except for the ductility transition which occurred approximately 50 F degrees lower for the tension impact tests with both heat treatment conditions. These data are compared in Table 4.

The measured areas occupied by the slag discontinuities in the gage cross section were found to range between 6 and 14 percent. The fracture appearance with slag discontinuities is shown with the fracture energy-temperature curve in Figure 9. The tensile fracture energies above the CFTT were decreased to 40 percent that of the sound steel material for the normalized and tempered condition as also was observed for the bending tests. The fracture energies were more sharply reduced for the specimens with slag inclusions in the quenched and tempered condition as tension tested; these fracture energies were lowered to approximately 30 percent of that obtained with the sound material.

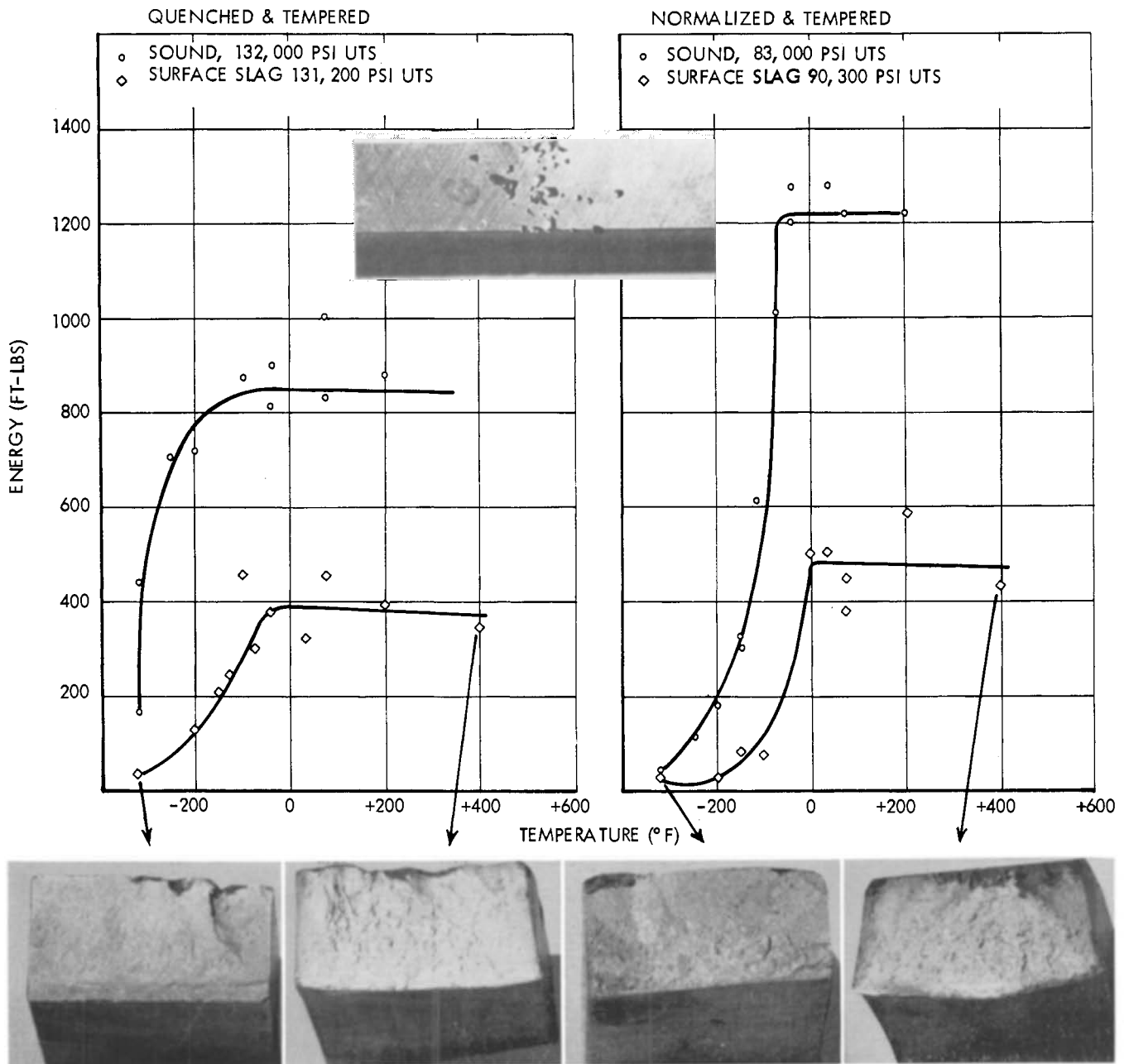


Figure 8—Bending impact test results with surface slag inclusions.

Hot Tears

The fracture energies for the bending test bars above the CFTT dropped sharply to about 25 to 30 percent that of the sound material. Since neither position nor degree of severity of the hot tears could be controlled during the casting process, approximately 70 specimens for each structure condition were tested to establish trends. The hot tear areas were measured on the ruptured faces and were found to occupy 5 to 40 percent of the specimen section. An example of brittle and ductile fracture appearance for bending impact is shown in Figure 10 for both heat treatments. The scatter obtained with the fracture energies is

apparent. The magnitude of the fracture energy values obtained at a constant temperature are functions of both defect size and position of the hot tear with respect to the striker anvil. The higher impact values were invariably obtained for the specimens with the hot tear discontinuities at positions away from the area of the striker impact. This result is to be anticipated since both the tensile stresses and the rate of load application diminishes as the distance from the striker increases. The results show, therefore, that when located at the positions of high stress, hot tears are highly detrimental. The ductility and fracture transitions were observed to occur at sub-

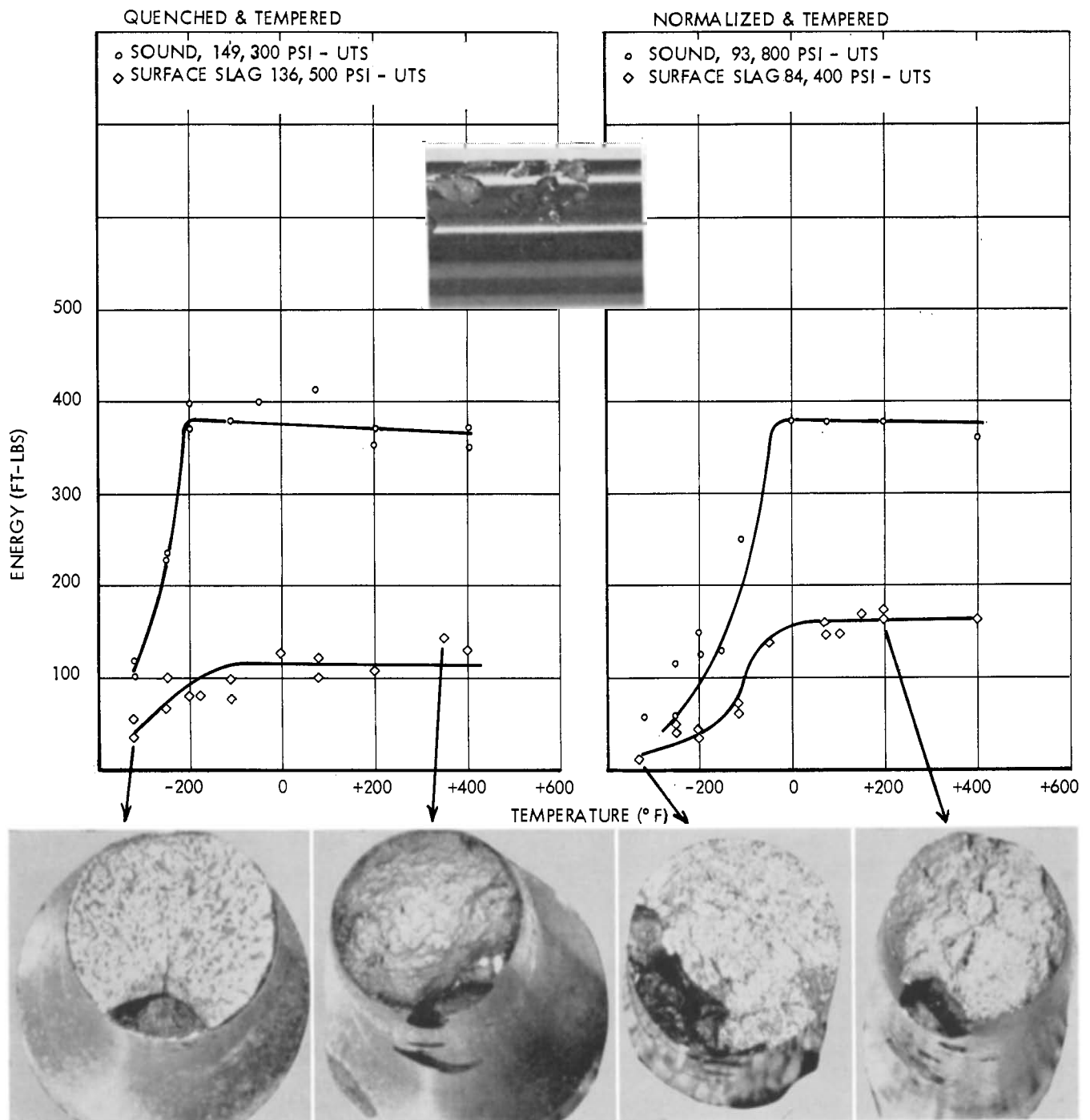


Figure 9—Tension impact test results with surface slag inclusions.

stantially higher temperatures than recorded for the sound bars as is shown in Tables 4 and 5. However, the transition temperatures did not exceed that of the tests with the Charpy V notch bars.

The impact data obtained for the hot tear tension impact specimens shown in Figure 11 appear more reproducible. Measurements made of hot tear discontinuities on the fractured faces revealed the initial crack depths to be within

0.030 to 0.040 inch from the surface while the area occupied by the discontinuity in the gage diameter was within the range of 4 to 10 percent. Tensile stock with larger hot tear discontinuities fractured during the specimen machining operation. The magnitude of the stresses generated as a result of the grinding operation was apparently sufficiently high to induce failure of those bars containing hot tears greater than some critical size. The machining operation conse-

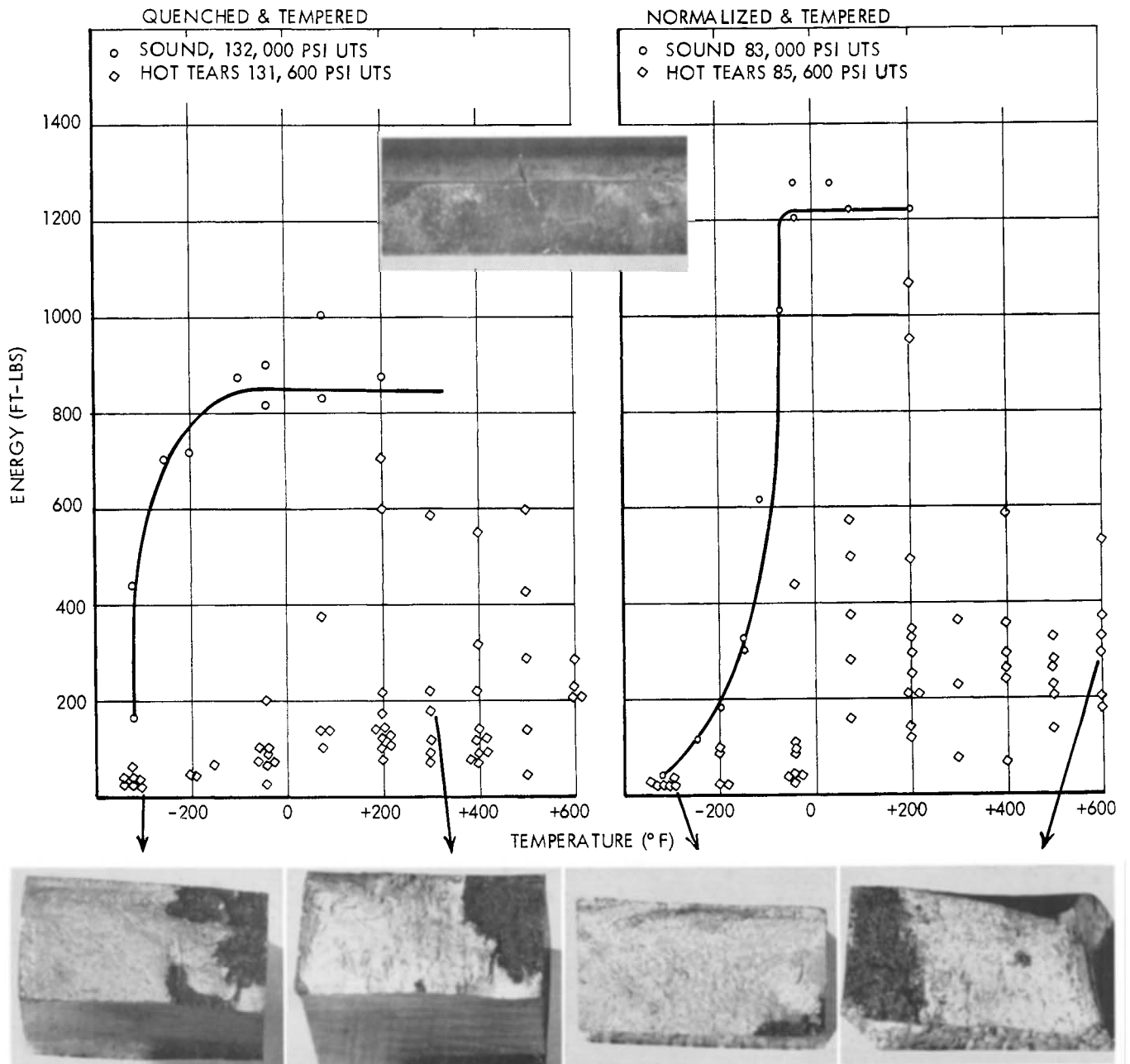
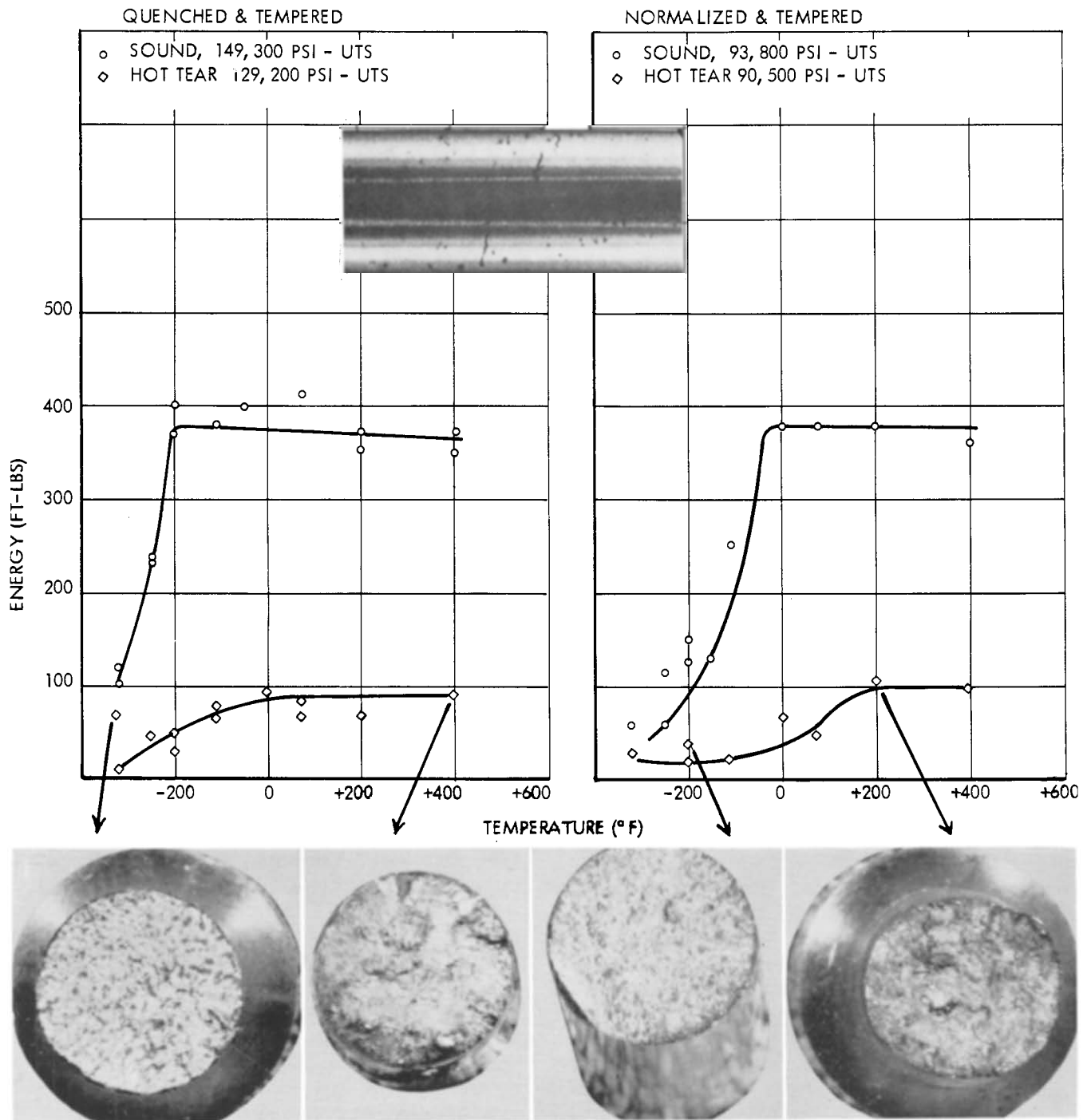


Figure 10—Bending impact test results with hot tear discontinuities.

quently provided an indirect screening of the magnitude of the hot tears which were tested. The transition from brittle to ductile fracture for tension impact also shifted to higher temperatures for both heat treatments as compared to the sound steel, as shown in Figure 11. The fracture energy above the CFTT was reduced to 20 percent of that of the sound steel. The CFTT was observed to occur for both the tensile and bending impact tests at approximately 50 F degrees above that of sound steel for the quenched and tempered specimens and 200 F degrees above the sound steel for the normalized and tempered condition.

The hot tear discontinuities had the most deleterious effects on the impact properties of the casting discontinuities investigated. Since surface notch acuity is a primary factor in controlling crack formation and propagation, this effect is not surprising." However, it might also be anticipated that the transition range would be higher than observed for the Charpy V notch testing. This was not the case and the reason could be attributed to crack depth and possibly other

* Note—Entire cross section is uniformly stressed internally on tension impact testing.



metallurgical variables, such as the decarburization at the surface of the hot tear.

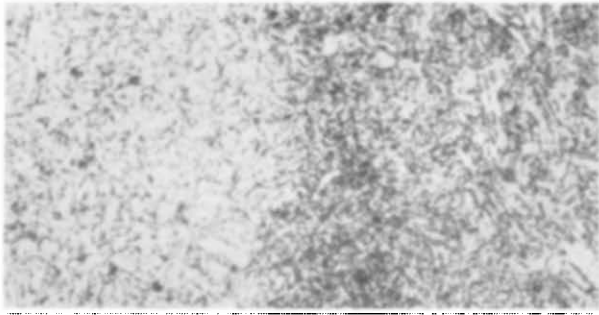
Welded Cast Steel

Typical microstructures obtained for the fully heat treated weldments are shown in Figure 12. The as-welded structure for cast steels is readily discernible and normally consists of three regions: the weld metal, a coarse grained heat affected zone

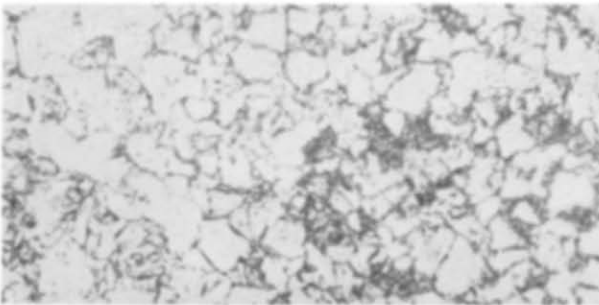
and the structure of the base metal cast steel. The beneficial effect of the heat treatment is a homogenization of the structure in which these zones are no longer as clearly discernible. The weld material appears slightly coarser grained than the cast steel for both the quenched and tempered and normalized and tempered heat treatments. Some trace of the heat affected zone is shown for the quenched and tempered bending specimen weldment.

WELD

BASE METAL



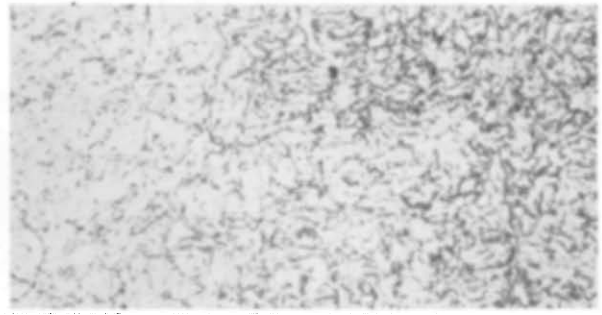
A) Q & T BENDING SPECIMEN
METAL ARC-COATED ELECTRODE



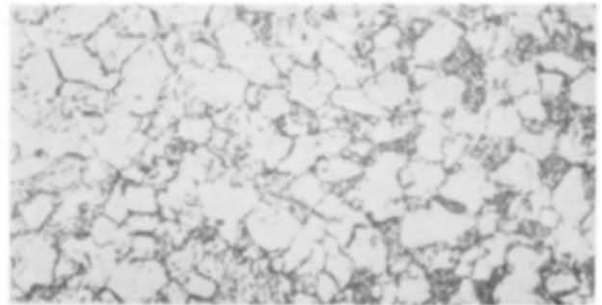
B) N & T BENDING SPECIMEN
METAL ARC-COATED ELECTRODE

WELD

BASE METAL



A) Q & T TENSION SPECIMEN
TIG - BARE ELECTRODE



B) N & T TENSION SPECIMEN
TIG - BARE ELECTRODE

Figure 12—Microstructure of the (a) quenched and tempered and (b) normalized and tempered Ni - Cr - Mo (8630) cast steel showing the weld area 500X.

The appearance of the weld in the tension bar specimen is somewhat more uniform than in the bend tests. It was noted earlier that different welding techniques were used for the tensile specimens than for the bending specimens. The former were welded with uncoated electrodes under an argon atmosphere using the tungsten inert gas (TIG) process while for the latter the specimens were metal arc welded in air with coated electrodes. The filler weld rod material was of slightly different composition for the two welding techniques. For normalized and tempered specimens, the weldments appear similar, exhibiting a transition which occurs from the weld zone of predominately ferrite to the base metal that contains an increased amount of pearlite.

The energy-temperature curves for impact testing with the sound welded specimens are shown in Figure 13. The weld discontinuities are compared to machined sound weldments in each case. Ductility, fracture appearance, and impact energy data are given in the tables in Appendix I. A summary of transition data is shown in Table 5. The severity of the various weldment discontinuities are shown rated according to ASTM specifications in Table 3.

Sound, Machined Welds. . . Sound weldments were machined to remove the weld reinforcement to the uniform thickness of the cast steel plates. The bend test results indicated the quenched and tempered sound machined weldments developed impact energies greater than observed for the sound cast steel. The impact energy transition curves are compared in Figure 13. This behavior is attributed to the response to heat treatment of the weldments. Hardness measurements traversing the weld section showed an average BHN of 225; the equivalent tensile strength is approximately 120,000 psi. The cast steel hardness was measured to be 285 BHN; the ultimate strength is 132,000 psi as recorded in Table 1. Because of the lower strength level of the quenched and tempered weldments as compared to the cast material, the increase in impact toughness would be an expected occurrence. The transition data were similar ; the ductility transition is slightly lower for the cast steel while the CFTT was approximately 50 F degrees lower for the welds.

The transition temperatures for the cast steel and the welded cast steel in the normalized and tempered condition were also similar; the cast steel exhibited a slightly lower ductility transition

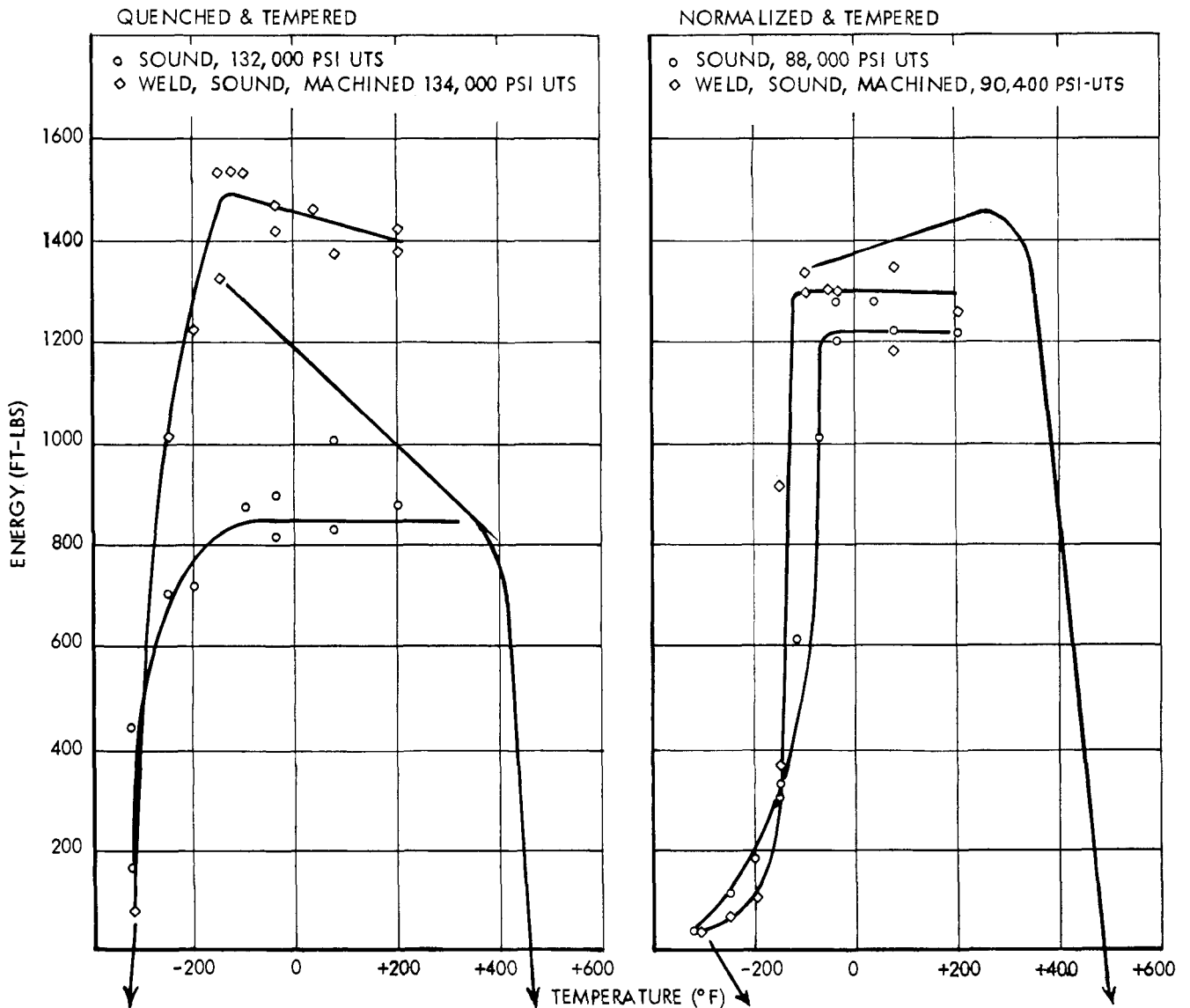


Figure 13—Bending impact test results of sound cast steel and sound welded, machined cast steel specimens.

by 50 F degrees and the welds had a lower CFTT by 50 F degrees. The impact fracture energies for the welds and cast steel were equivalent.

The welded, machined tensile impact specimens in neither the quenched and tempered nor the normalized and tempered condition developed ductile fracture energies as high as recorded for the sound cast steel. The curves are compared in Figure 14. Fracture energies above the CFTT

for the welded cast steel, however, were within 80 percent of the sound cast steel. Similar response of the welded cast steel to heat treatment as compared to the cast steel was observed as indicated by hardness measurements. The transition temperatures for the normalized and tempered welded cast steel varied only slightly from that of the cast steel. By some criteria, the cast steel provided lower transition temperature and by other criteria, the transition occurred at a

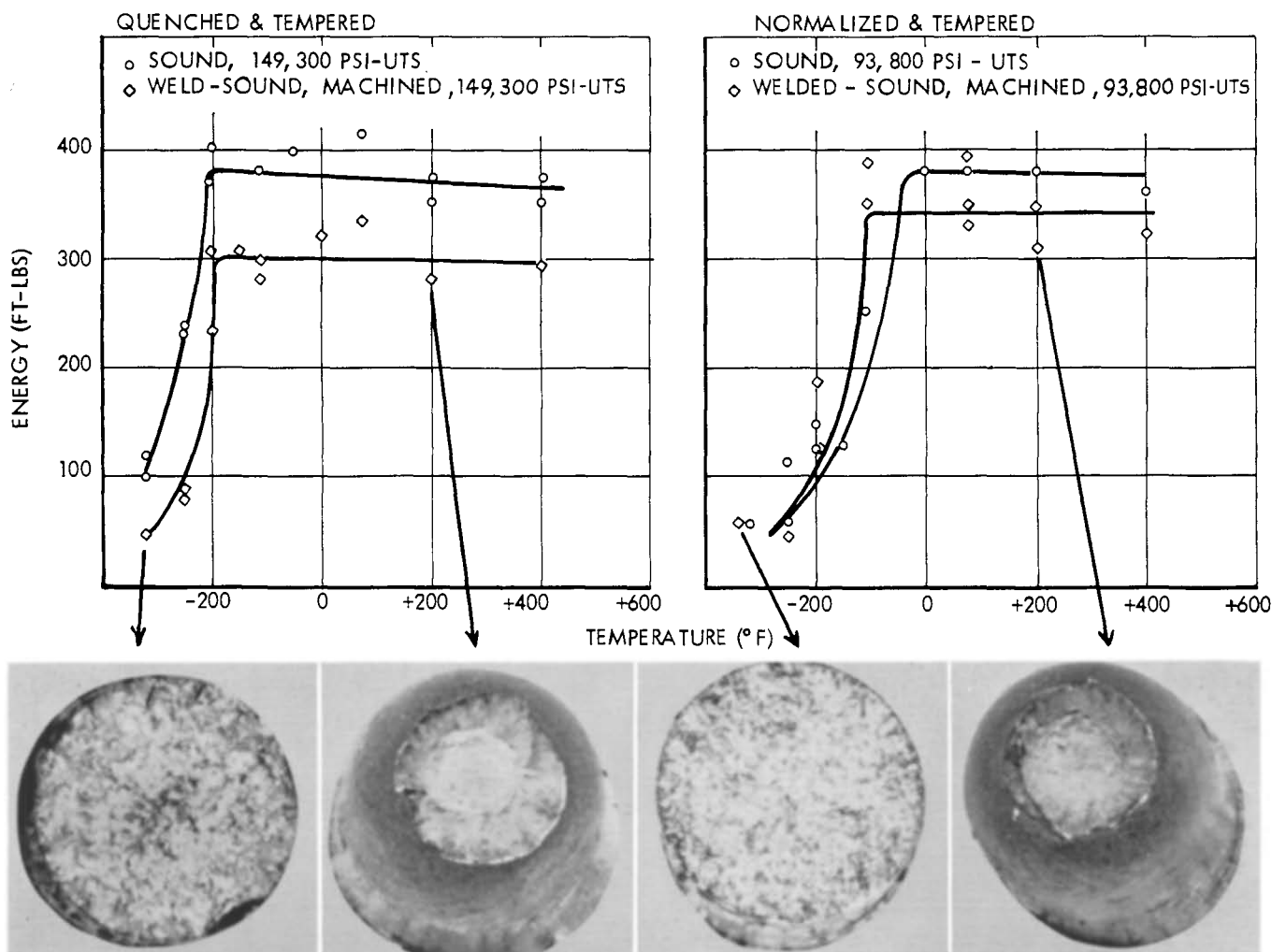


Figure 14—Tension impact test results of sound cast steel and sound welded, machined specimens.

lower temperature for the welded and machined cast steel. The fractures for both the bending and tension test bars occurred through the weld metal and not at the heat affected zone.

Sound, As-Welded..... The sound, as-welded cast steel test bars contained the reinforcing welds in place during testing. This condition resulted in a position of stress concentration at the juncture of the weld and the cast steel. The sound, as-welded bending test bars for the quenched and tempered condition displayed no change in transition temperatures as compared to sound machined welded cast steel. However, slightly lower fracture energies above CFTT were recorded as shown in Figure 15. The fractures were observed to initiate at the surface juncture of the weld bead and the base metal, suggesting a mild notch effect from the weld reinforcement. However, for the normalized and tempered condition, no significant changes in either the transition temperatures or impact energies above CFTT were observed be-

tween the as-welded and as-machined weld bending impact results. Similarly for the tension impact testing, no variation in transition temperatures was observed from the as-weld surface condition. Fracture energies measured for the as-welded cast steel, as shown in Figure 16, displayed a decrease for both heat treatment conditions because of the mild notch caused by the presence of the weld bead. The weld fracture for the tension bars was also observed to occur at the weld deposit-cast steel interface at the location of the stress concentration resulting from the mild notch.

Weld-Slag Inclusions . . . A sharp decrease in the bending impact properties resulted from the presence of slag inclusions. The impact energies for the quenched and tempered bending bars were reduced to approximately 35 percent that of the sound welds as shown in Figure 17. The entire transition range was shifted to higher temperatures by about 125 F degrees. The location of the discontinuities in the fracture faces, as shown

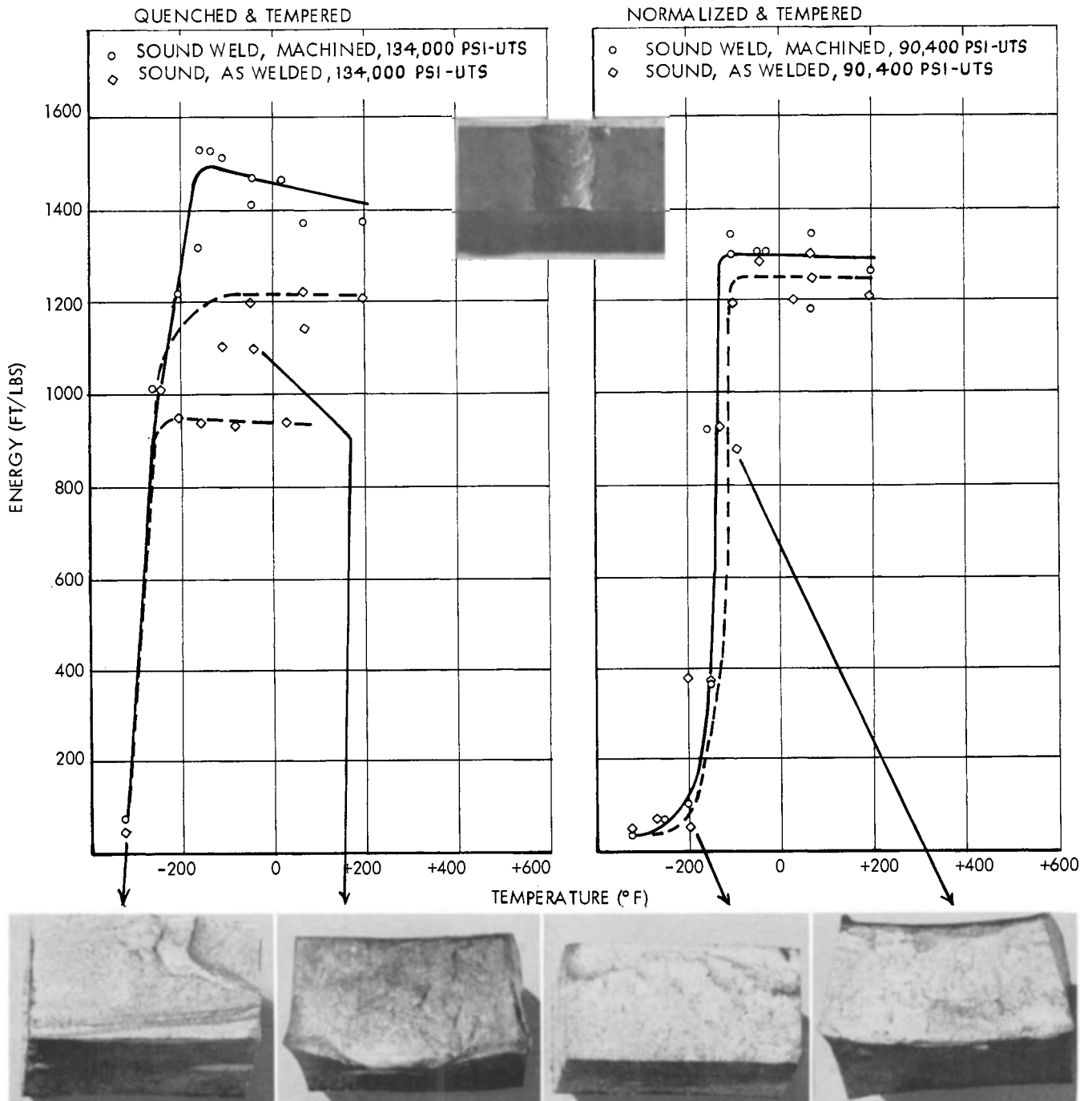


Figure 15—Bending impact test results of sound, as-welded specimens.

in Figure 17, are approximately midway between the neutral axis and the maximum stressed outer surface fibers. The area of the slag inclusions in the specimen cross section ranged between 12 and 18 percent. Normalized and tempered welds containing slag were not as severely affected as the higher strength cast steel. The ductility transition was not affected; however, the .5FTT and CFTT shifted upward by about 100 F degrees. The fracture energies above CFTT were reduced to about half of that of the sound welds.

Slag weld inclusions in welded cast steel were found to be detrimental when loaded in tensile impact. The fracture energies dropped to one third of sound weld values (QT) and the entire transition was shifted upward by approximately 150 F degrees. The fracture energy transition curves are shown in Figure 18. The shift in transition for the normalized and tempered, heat treated cast steel was 100 F degrees or somewhat less. The fracture energies above the CFTT were reduced to about half of that of cast steel with a

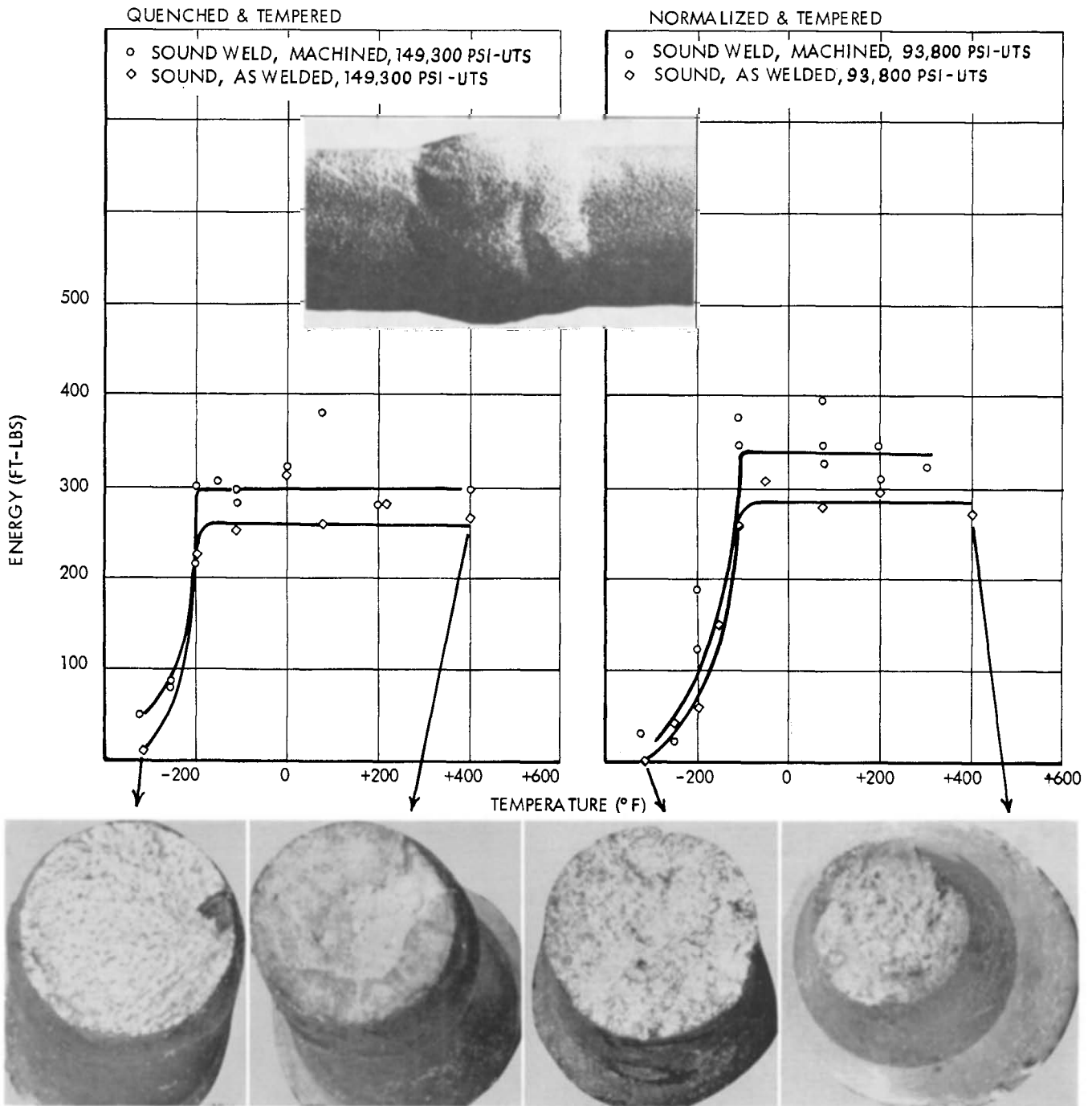


Figure 16—Tension impact test results of sound, as-welded specimens.

sound weld. The slag inclusions occupied from 8 to 17 percent of the gage diameter.

Weld Undercut. . . Weld undercut represented a severe condition for bending impact tests. The energy transition curves as shown in Figure 19 indicate the fracture energies above the CFTT for welds containing undercut discontinuities to be approximately 35 percent (QT) and 40 percent (NT) as compared to sound welds. The entire transition range for both heat treatment condi-

tions was shifted to higher temperatures: 125 degrees F (QT), 75 degrees F (NT) . The undercut discontinuity occupied an area of 7 to 10 percent of the gage cross section.

The notch effect produced by an undercut in the welded tension bars was evidently not as severe as that of the slag inclusions. The energy transition curve shown in Figure 20 indicates the fracture energies above CFTT to be approximately two-thirds that of the sound tensile weldments

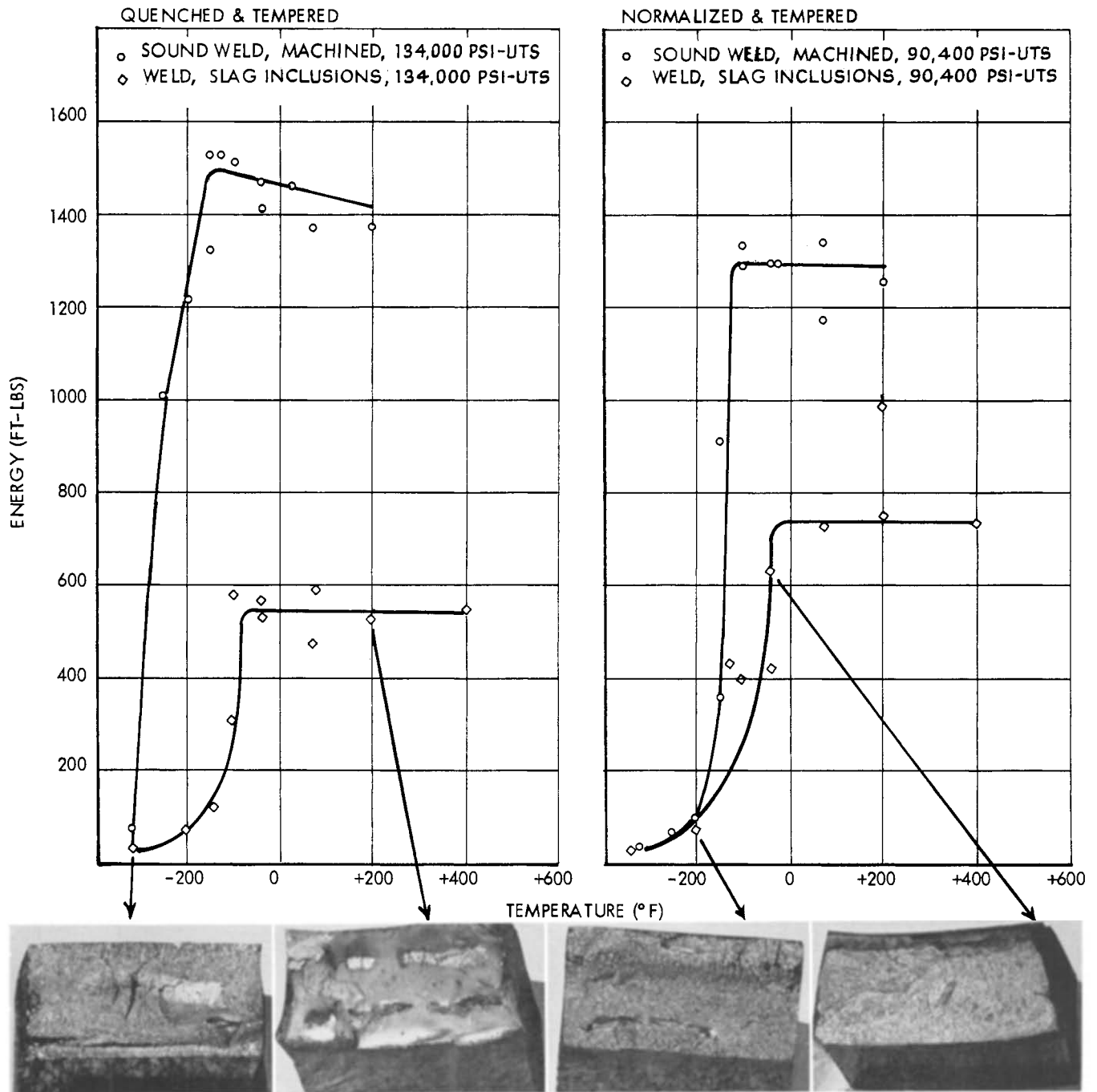


Figure 17—Bending impact test results with weld, slag porosity discontinuities.

for both structure conditions. A linear shift upward of 50 F degrees was observed for all transition temperatures for the quenched and tempered condition. For the normalized and tempered welds the CFTT was unchanged. However, a 50 F degree shift to higher temperatures was observed for the ductility transition and the .5FTT. The area occupied by the undercut was measured to be 6 to 15 percent.

Weld-Incomplete Penetration . . . Incomplete penetration between the weld metal and the cast

steel plate appeared to be the least severe weld discontinuity for both the bending and tension impact testing. Nevertheless, incomplete penetration was detrimental to the impact properties of the steel, as indicated by the energy transition curve for the bending tests shown in Figure 21. The fracture energy above CFTT was reduced to less than half of that of sound welds for the quenched and tempered heat treatment while for the normalized and tempered incomplete weld penetration test, the reduction was less severe

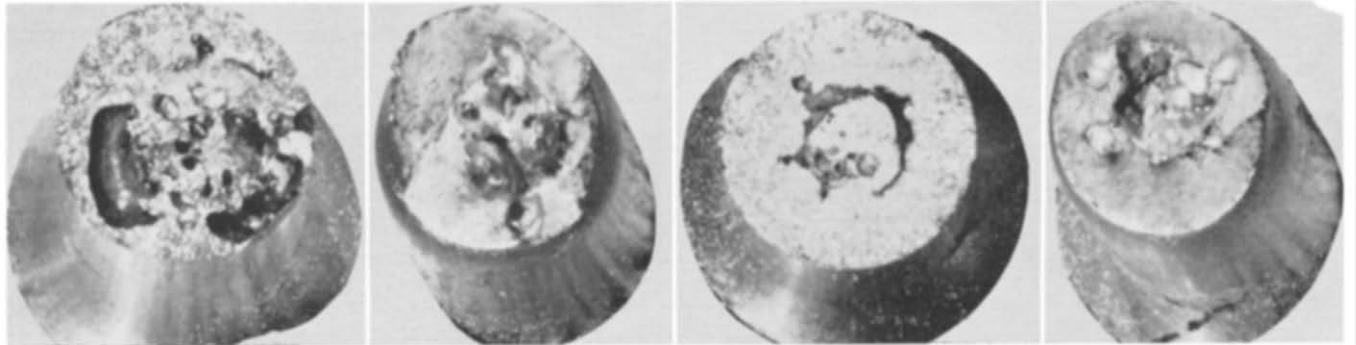
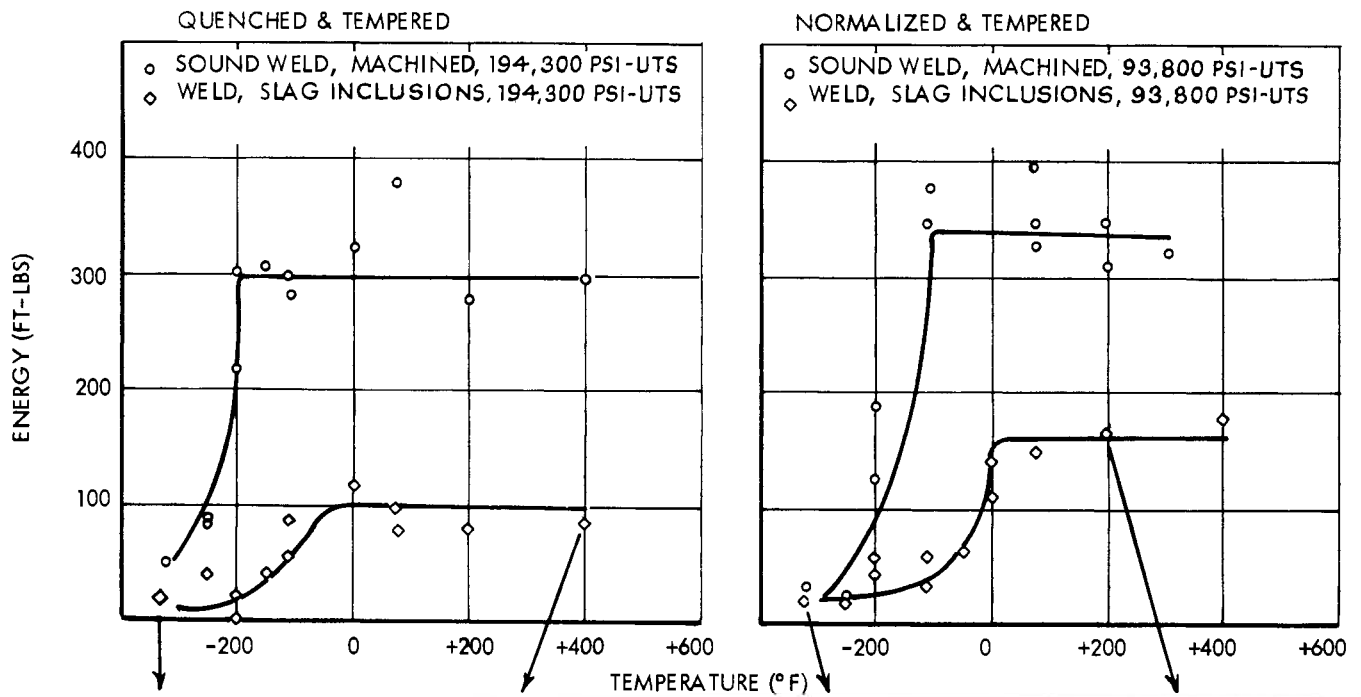


Figure 18—Tension impact test results with weld, slag porosity discontinuities.

but was still only about 60 percent of that of the sound welds. The upward shift in transition was nearly 50 F degrees for both heat treatments. The area of incomplete penetration, as measured in the fracture face, was 9 to 15 percent. For the tension impact bars the incomplete penetration area in the gage diameter was 4 to 6 percent. The reduction in fracture impact energies, as shown in Figure 22, is not very severe. The fracture energy developed above the CFTT is approximately 75 percent that of sound welds for both structure conditions. An upward shift of approximately 50 F degrees of the transition for the quenched and tempered cast steel is apparent. Incomplete weld penetration discontinuity did not affect the CFTT for the normalized and tempered steel; the ductility transition and .5FTT, however, did shift upward about 50 F degrees.

Metallography

The microstructure of the cast steels after normalizing and tempering is a mixture of ferrite

and pearlite and tempered martensite in the case of the quenched and tempered steels. The microstructures adjacent to the discontinuities were examined to ascertain whether any structural differences were discernible. Evidences of decarburization to varying degrees were found for the casting discontinuities of gas cavities, slag inclusions and hot tears. The depth of decarburization around the gas cavities varies from 5 to 10 mils for the sample investigated. The example shown in Figure 23 shows a decarburized layer of approximately 5 mils adjacent to the pinhole. The slag inclusion in Figure 23 shows a carbon depletion of approximately 10 mils. Cracks are shown emanating from the slag inclusion into the ferrite region with one crack terminating at the ferrite in a region containing pearlite. The depth of decarburization found with hot tears varied for the specimens examined from 3 to 7 mils for the bending impact bars and 1 to 3 mils for the tension impact bars. The amount of decarburization increased with crack width.

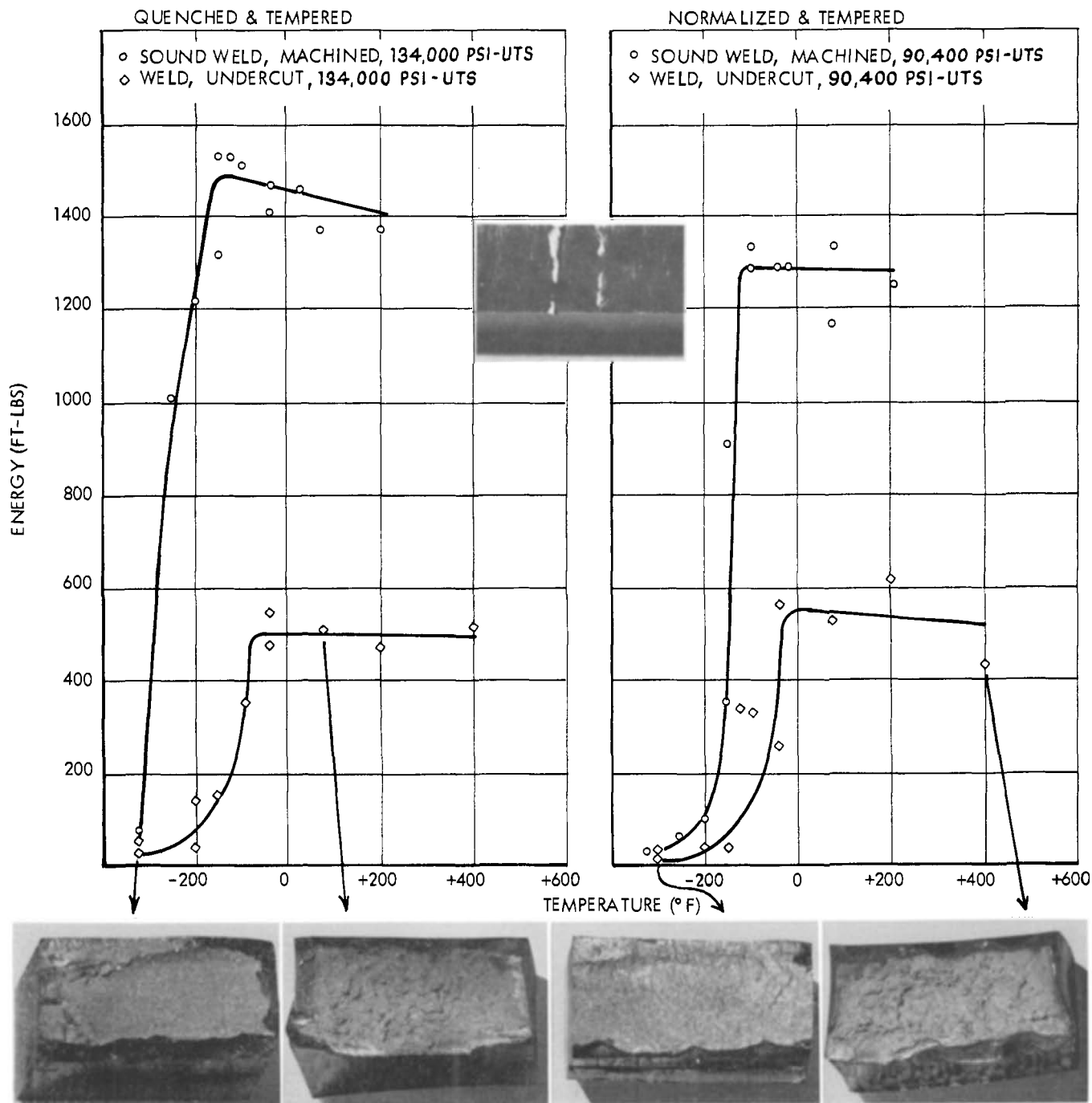


Figure 19—Bending impact test results with weld, undercut discontinuities.

Decarburization was also detected in the weld discontinuities of undercut, incomplete penetration and slag. The decarburized layer for the weld undercut was observed to be approximately 2 mils. Decarburization depth for the incomplete penetration was measured to be 3 to 5 mils, as shown by the example in Figure 24. Regions around the weld slag show decarburization to a lesser extent. Thin regions of ferrite are shown outlining the slag inclusions in the illustrations of Figure 25. A crack is indicated originating at the slag

stringer through a decarburized region into the surrounding tempered martensitic microstructure.

Decarburization is found in only the discontinuities that have access to the surface of the specimen with the decarburization taking place during heat treatment. Extensive decarburization has been observed to affect mechanical properties of steel. The ultimate tensile strength of steel is reduced because the areas depleted of carbon do not possess the strength of the unaffected regions. Only limited information is

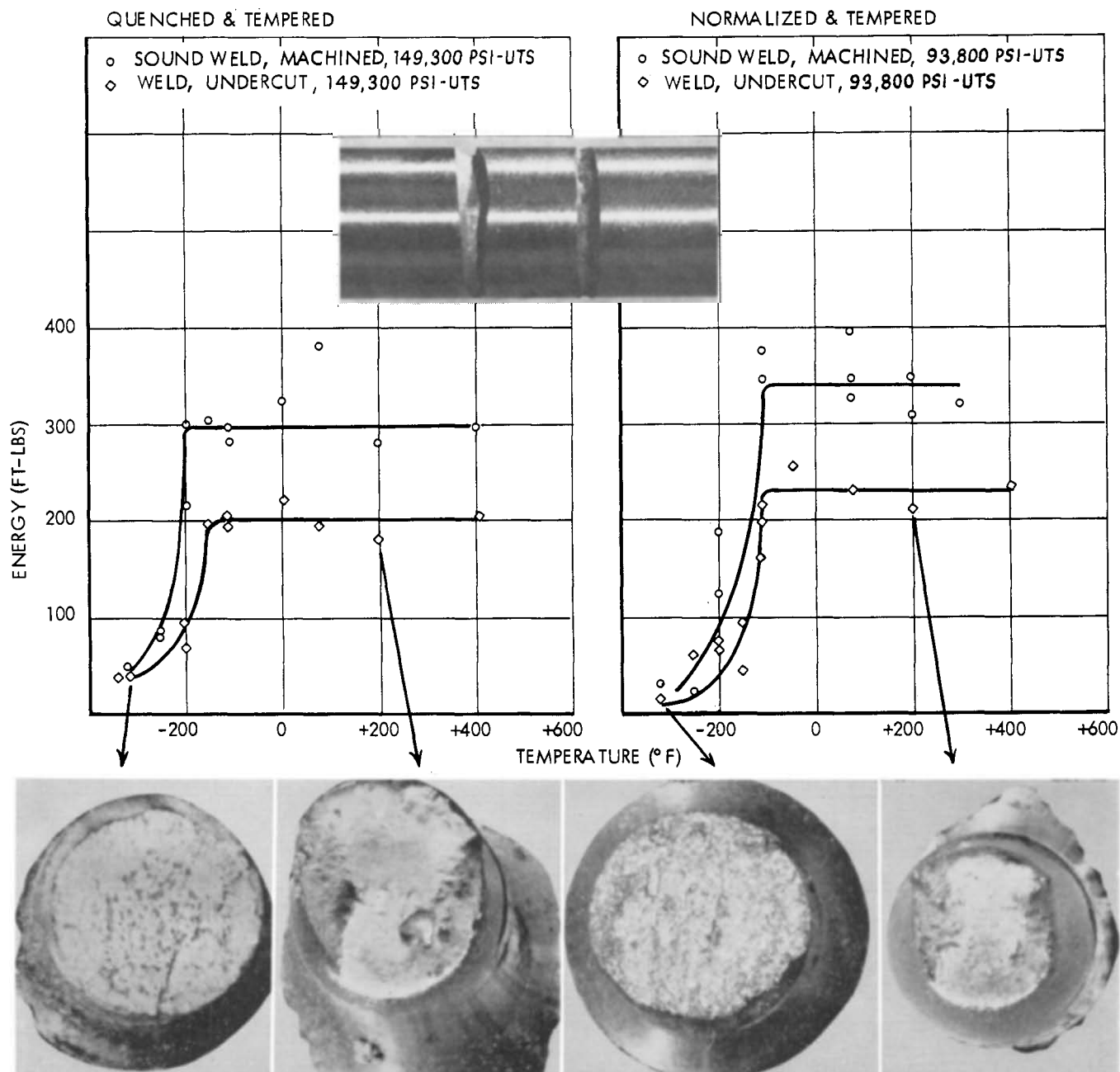


Figure 20—Tension impact test results with weld, undercut discontinuities.

available on the effect of decarburization on impact resistance. One study (32) on several alloy steels showed that the presence of a decarburized layer in an edged notch sheet specimen tested in tension provided an increase in notch tensile strength compared to steel without decarburization. This increase was attributed to the influence of decarburization on crack initiation requirements. The percent of shear in the fracture increased only slightly indicating that crack propagation was little affected. Notch strength was found to increase with greater depths of decarburization. A decarburized zone adjacent to a

stress raiser has a similar effect during impact testing.

The impact test is conducted under conditions in which the maximum load applied is sufficient to produce failure. The existence of a decarburized steel layer at the point at which the failure would normally be initiated will result in an increase in the amount of energy absorbed during this failure. Such a condition would exist if the steel at a discontinuity were decarburized or if the surface of a bending impact test were decarburized. The increase in the amount of energy

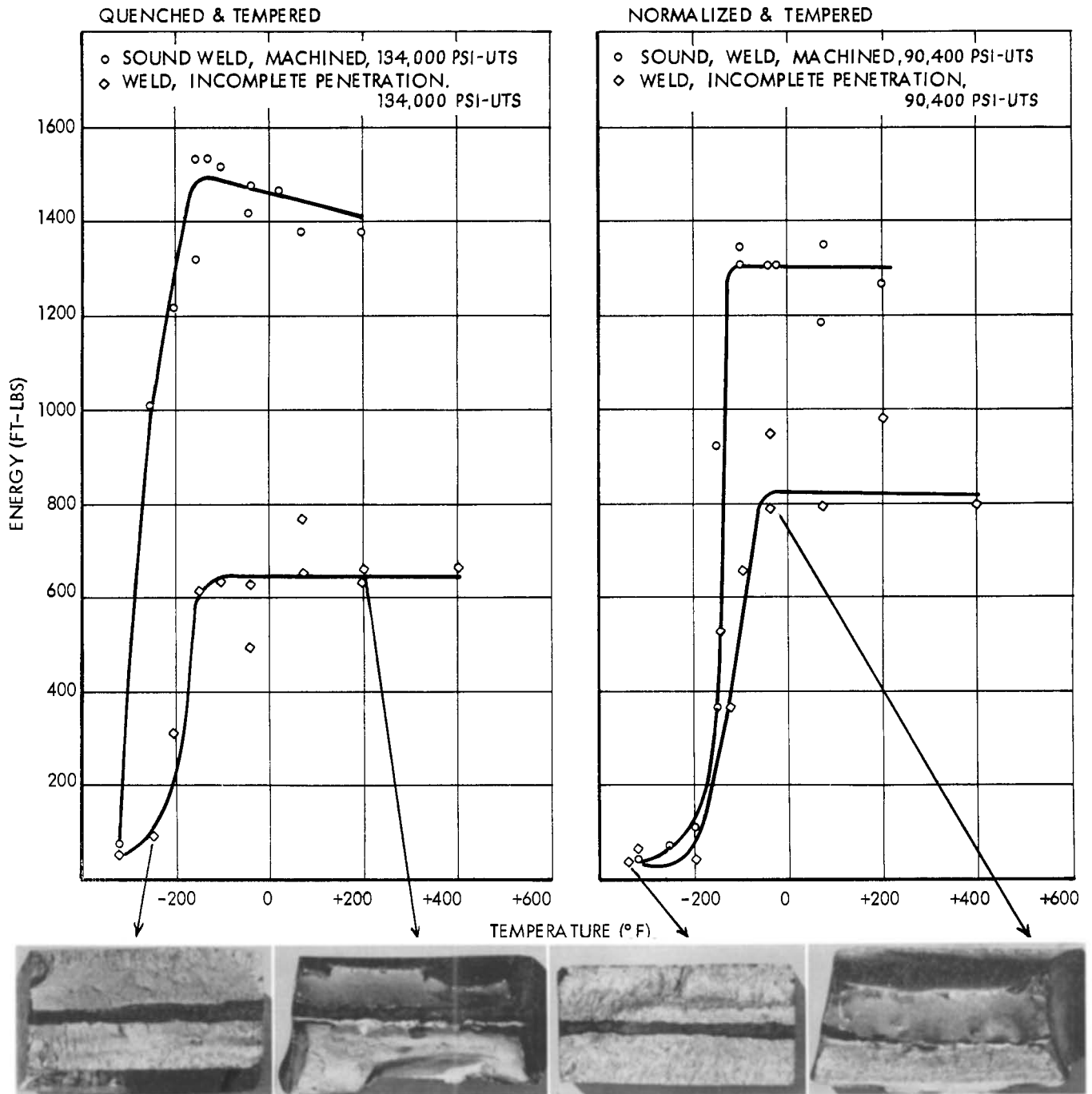


Figure 21—Bending impact test results with weld, incomplete penetration discontinuities.

absorbed during the fracture process would result because of the greater plastic deformation that occurred prior to initiation of cracking.

The existence of the decarburized layer at discontinuities can increase the degree of fibrosity in the fracture surface, thereby resulting in a lowering of the fracture transition temperature. This lowering occurs because the plastic deformation at the discontinuity reduces the notch acuity. Also a relaxation of the degree of stress triaxiality

occurs when compared to a similar test section where no decarburization was present and the metal at the discontinuity was at full strength. This effect would explain in part the lower fracture transition of the hot tear discontinuities tests as compared to the Charpy V notch specimens.

Ductile Fracture

Measured ductilities at temperatures above where the fracture appeared (CFTT) were observed to vary in several ways. First, the ductility

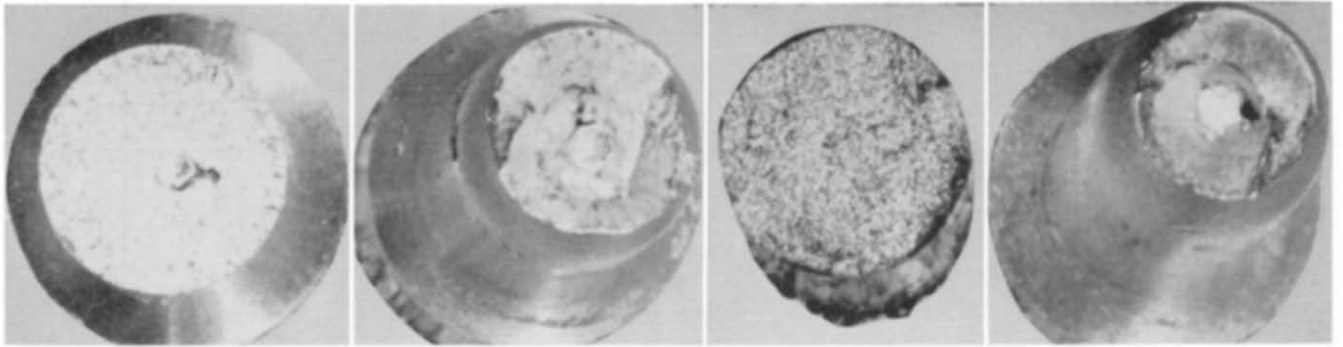
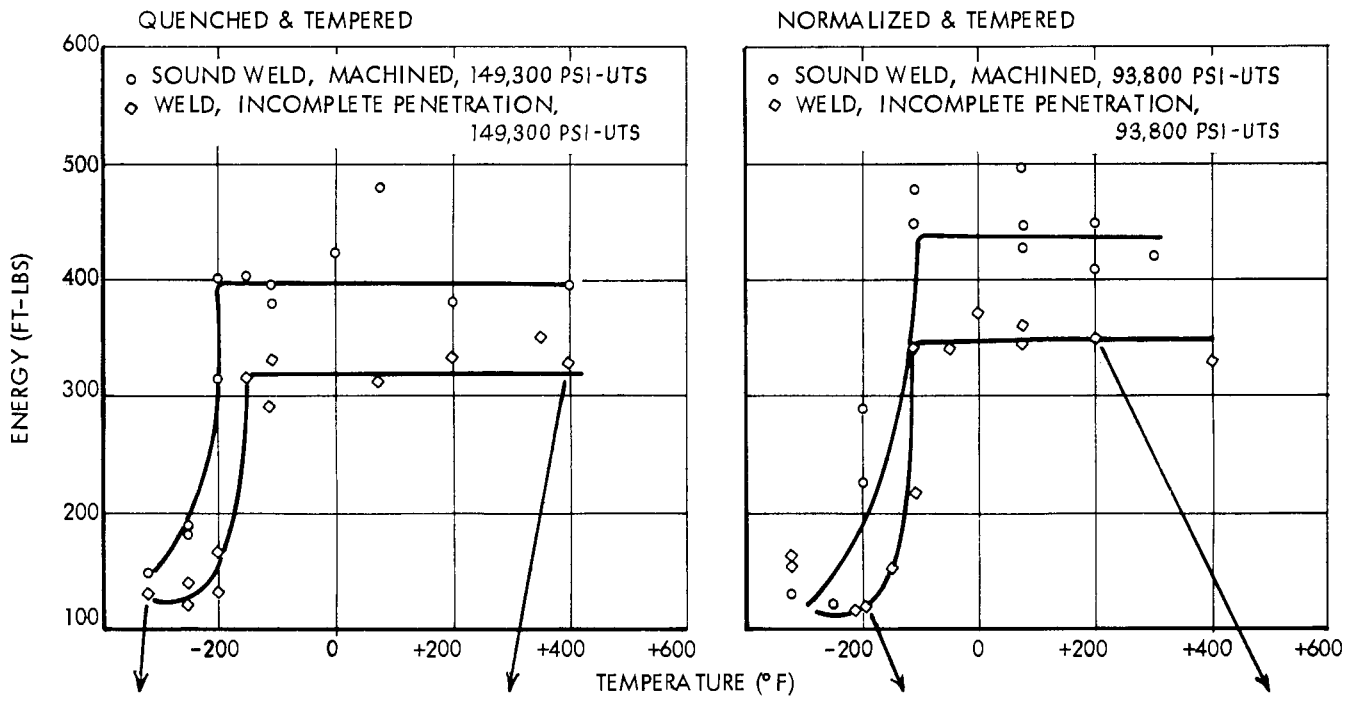
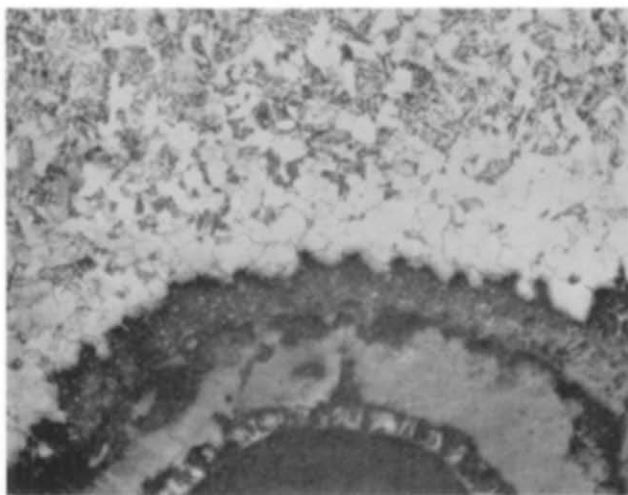
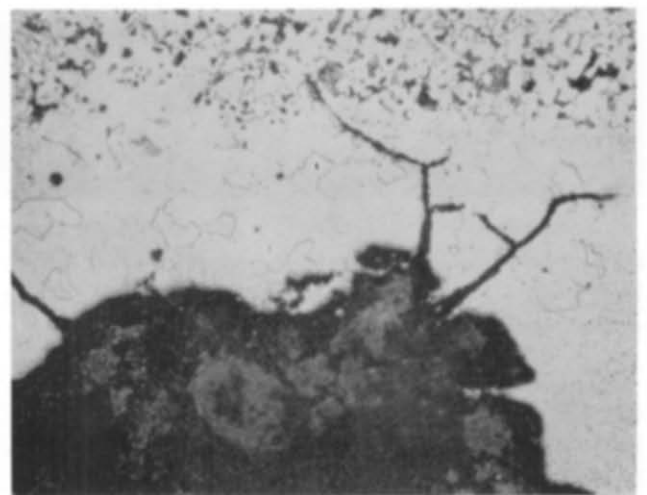


Figure 22—Tension impact test results with weld, incomplete penetration discontinuities.



(a) bending test specimen, cavity, NT



(b) bending test specimen, slag inclusion, NT

Figure 23—Examples of decarburization found adjacent to (a) cavity and (b) slag inclusions of cast steel.

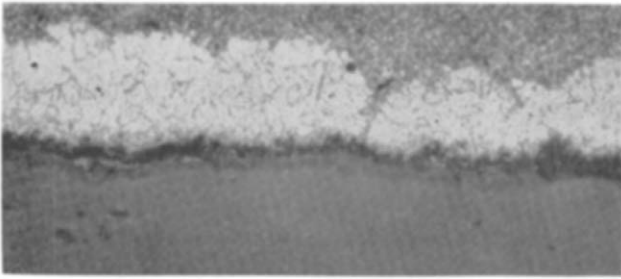


Figure 24—Example of decarburized layer in incomplete penetration weld 150X (dark area is mounting material in the incomplete weld penetration area).

measurements for various heat treatments showed that the ductilities of steels in the normalized and tempered condition were substantially higher than for the quenched and tempered condition. However, there exists a greater amount of plastic deformation in the lower strength normalized cast steel at test conditions above the ductility transition.

A comparison of the ductilities for the various casting discontinuities and the weld discontinuities in cast steel showed a variation of ductility in a regular manner with the energy required for rupture. The bending impact ductilities were measured by maximum lateral contraction on the tensile side of the test specimens; while for the tension impact test, elongation in the 1.4-inch long gage and reduction in area were measured.

The tensile failure above the ductility transition occurred by the shear mode and produced a necked region with the typical cup-cone fracture appearance. The effect of discontinuities was a localization of the necked region at the position of the controlling discontinuity. This effect is similar to machining a necked region or reduced area into the gage section prior to testing. It follows that during the testing, the plastic deformation is localized and necking will occur early; consequently, the accompanying longitudinal elongation is not uniform along the gage length but is restricted primarily to the cross section in the vicinity of necking. The radius of curvature of the necked region results in a stress concentration in the necked region leading to a relatively diminished ductility and a lower energy fracture. (33) This fact implies that the energy absorbed during ductile failure is related to the effective volume undergoing plastic deformation.

A similar study showed the energy absorbed was related to the gage volume. (34) Specimens of the same material were tested with 1/2 inch diameters but of two gage lengths: 2.5 inches and 5.0 inches. The shorter gage absorbed 1300 ft. lbs. of energy and broke; the longer specimen

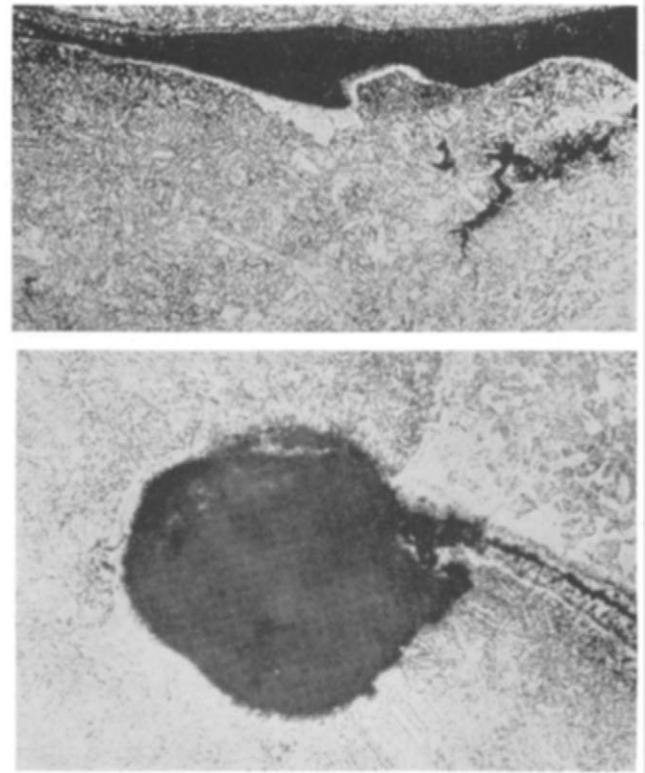


Figure 25—Examples of decarburization found adjacent to weld slag porosity for quenched and tempered tension tests specimens.

absorbed 2100 ft. lbs. of energy and did not break.

This trend of the effective volume undergoing plastic deformation as the primary control of the energy absorbed for ductile fracture is reflected in the ductilities recorded for both the tension and bending specimens. The data show that lower ductilities were invariably associated with the lower fracture energies while with higher ductilities, the fracture energies increased. The highest energies and corresponding highest ductilities were recorded for the discontinuity free unnotched test specimens.

Brittle Fracture

The fracture energy (E) at any temperature on the transition curve consists of the sum of the energy to initiate a crack (E_i) and the energy to propagate the crack (E_p):

$$E = E_i + E_p$$

Several investigators have shown that very little energy is required to propagate a crack by cleavage and the elastic strain energy available in the vicinity of the crack tip is sufficient to sustain fracture. It has been determined (35) that the plastic work contribution in the brittle fracture of a ship steel broken at room temperature

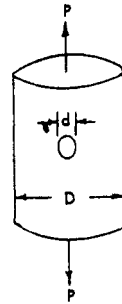
TABLE 6
Estimation of K_t

was of the order of 5 ft. lbs. per square inch or approximately 0.5 ft. lb. in the case of the tension impact specimens, if the fracture made is actually cleavage. An analysis of the energies recorded in the brittle region for the tests of this report shows that a negligible portion of the total energy is absorbed to provide work of plastic deformation and that nearly all the energy is expended for fracture initiation, or $E \sim E_i$ near the ductility transition temperature (DTT). Since negligible gross plastic deformation occurs during cleavage fracture, the nominal stress for fracture can be calculated by dividing the maximum stress resulting from stress concentration by the stress concentration factor.

The maximum normal stress theory which has been found applicable as a criterion for brittle fracture (36) states that when one of the principal stresses reaches a critical value, brittle failure will occur. The energy necessary for brittle fracture is inversely proportional to the square of the stress concentration factor. A knowledge of the stress concentration factor (K_t) was therefore necessary to determine the energy required for brittle fracture. The various shapes of the discontinuities were measured and to a large extent idealized to obtain an approximation of K_t from compiled stress concentration design data. (36, 37) Values of K_t were taken directly from stress concentration curves or were obtained by estimates based on the curves and shapes of discontinuities. The manner of estimation is shown schematically together with the source from which the K_t values were selected in Table 6.

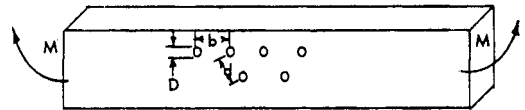
The stress concentration produced by the cavity machined in the tension impact tests to simulate gas cavities was readily obtained, since the 1/16 inch diameter hole was artificially produced by machining and was therefore a constant dimension and location. The K_t value obtained for the tension impact cavity was 1.93. Determination of the stress concentration value for cavities in bending impact was more involved since the size, shape and distribution were all variables. A circular shape for the cavities was assumed and from a series of measurements from various test specimens, a mean gas cavity diameter of 1/16 inch with spacings of 1/4 inch was selected. This method resulted in a stress concentration value of 2.3. If the gas cavity diameter and spacing increase proportionately, the K_t remains constant. However, if the spacing is increased for a constant cavity diameter, K_t will increase up to a maximum value of 3. (36) This example shows how discontinuity spacing can result in a substantial de-

Pinhole Tension



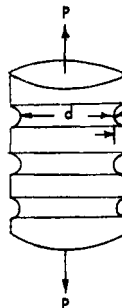
Solid circular shaft,
transverse hole - tension
Reference (36) pg. 226
 $d = 1/16''$
 $D = .357''$
 $K_t = 1.93$

Pinhole Bending



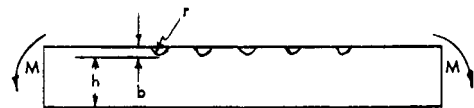
Flat plate, spaced holes - tension
Reference (36) pg. 267
 $D = 1/16''$ $d = 1/4''$ $D/b = .25$
 $b = 1/4''$ $K_t = 2.3$

Slag Inclusions - Tension



Solid circular shaft,
circular groove - tension
Reference (36) pg. 221
This estimate does not include any
stress relieving effect of adjacent
notches or filled cavities.
 $r = .015 - .060''$ $r/d = .046 - .250$
 $d = .327 - .237''$ $h/r = 1$
 $K_t = 2.2 - 1.58$

Slag Inclusion - Bending



Flat plate, hyperbolic groove - bending
Reference (36) pg. 251
This estimate does not include any stress relieving
effect of adjacent notches or filled cavities.
 $r = .015 - .060''$ $b = .015 - .060''$ $b/r = 1$
 $h = .485 - .440''$ $r/h = .031 - .137$ $K_t = 2.6 - 2.1$

crease in K_t and that the limiting value for stress concentration as produced by gas cavities is 3.

Stress concentration values were obtained for slag inclusions by assuming that the stress concentration produced by the continuous slag particles could be simulated by a hyperbolic groove as shown in Table 6. The stress concentrations for

slag inclusions are based on measured diameters and depths ranged from 2.1 to 2.6 for bending impact and 1.58 to 2.2 for tension impact. It is reasonable to assume that these ranges of K_t are conservative since the interaction of adjacent inclusions was not considered. The K_t value will increase sharply and will theoretically approach infinity as the inclusion particle size decreases or the section size increases. However, if the section size becomes smaller or the inclusion size becomes large, then the K_t value diminishes to a limiting value of approximately 1.4 for both bending impact and tension impact tests. (36) These relationships point out the strong influence section size and particle size may have on the fracture energy and why correlation between laboratory test data and actual failures of large components is different in many cases.

Hot tear discontinuities can be said to have essentially a zero radius of curvature at its extremity. Theoretically, as the radius approaches zero, the stress concentration approaches infinity. (38) As an approximation, K_t for hot tears was estimated at 10.

The fracture energies recorded for the various discontinuities at a constant temperature near the DTT are listed with the K_t values in Table 7. The temperature selected for the quenched and tempered cast steel was 200 degrees F and -150 degrees F for the normalized and tempered cast steel. The energy was plotted for particular discontinuities as a function of K_t^{-2} and is shown in Figure 26.

These data are only approximate values since the impact curves from which the energy near

TABLE 7
Summary Stress Concentration and Ductility Transitions Fracture Energies for Casting Discontinuities

Discontinuity	Estimated K_t	(K_t^{-2})	Q&T Impact Energy at -200°F (Ft.-Lbs.)	N&T Impact Energy at -150°F (Ft.-Lbs.)
Hot Tear				
Tension	10	0.01	45	20
Bending	10	0.01	70	50
Pinhole				
Tension	1.93	0.27	73	55
Bending	2.3	0.19	72	80
Slag Inclusions				
Tension	1.58-2.2	0.40-0.21	80	75
Bending	2.1-2.6	0.23-0.15	134	84

the ductility transition was obtained as well as the inherent approximations involved in the K_t values are a source of scatter. However, from these data some generalizations can be drawn: First, it can be seen that since the impact energy is inversely proportional to the square of the stress concentration factor (K_t^{-2}), the stress concentration exerts a very strong influence on the brittle fracture energy. Second, it would be anticipated from this relationship that for a higher K_t , the energy for brittle fracture would be reduced to a negligibly low or zero value and therefore, the straight lines drawn through the data points shown in Figure 26 should extrapolate to the origin. That this is not the case can be attributed partially to the mechanism of fracture and to the impact test itself. When a crack is propagating in a brittle manner some small finite energy must be supplied since, during the fracture process new surface is being created at the advancing crack tip. Further, since sliding contact is made between the bending specimen and the support fixture, work is expended during the impact test. The most significant factor is that kinetic energy is imparted to the tension impact

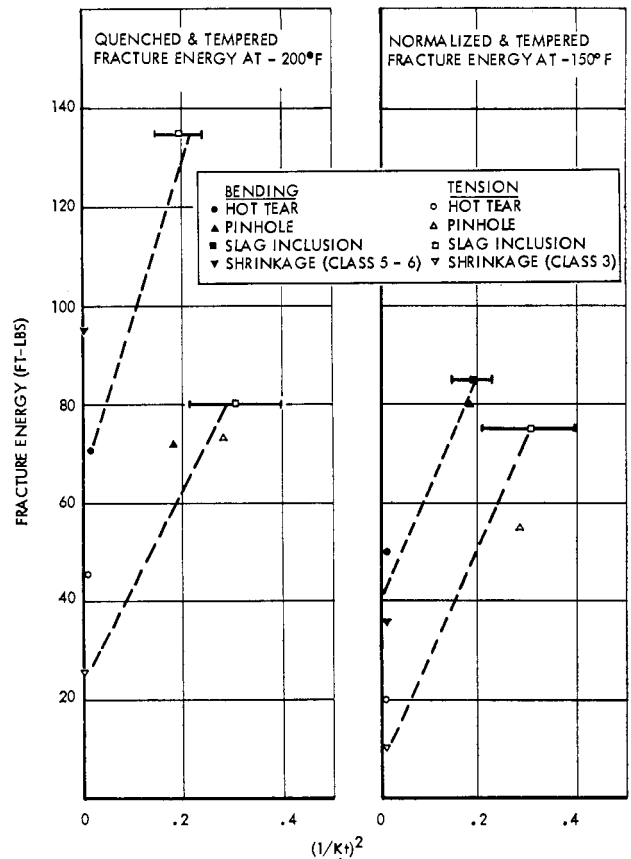


Figure 26—Relation of fracture energy at the ductility transition temperature to stress concentration for casting discontinuities.

and bending impact specimens and they are propelled at high velocities away from their initial rest position. For these reasons the straight lines drawn through the data points in Figure 26 intercept at some value along the energy axis. The intercept values for the bending impact tests are substantially higher than for the tension impact tests indicating the larger amount of energy expended in these various factors.

The data indicate that the higher stress concentrations produced by hot tears are more damaging to the impact properties than those produced by the gas cavity and slag discontinuities. When K_t values were estimated for the surface slag inclusions, the presence of the particle was not considered. Since the slag particles are weak and possess a low interfacial strength, the data suggest that the inclusion is an inert particle with respect to the fracture process. In other words, it is the shape, size and distribution of the surface voids produced by the slag particles and not the particle itself which determines the stress concentration value (K_t).

Lastly, the slopes of the curves in Figure 26 should provide information relative to cast steel fracture strength for two strength levels (heat treatment and microstructures) and impact tests. However, the slopes of the curves as drawn in Figure 26 show no significant differences.

Evaluation of the Research

The ability of a steel casting to withstand impact loading without failure is determined by a number of factors. These factors include the magnitude of the impact stress, the rate of loading, the ambient temperature, the presence of multiaxial stresses and the presence of stress concentrations. Other metallurgical factors such as the composition of the steel, its microstructure and strength level will influence the ability of cast steel to withstand impact loading.

This investigation utilizes three different types of impact tests to evaluate the effects of some metallurgical variables and the presence of different types of discontinuities that produce stress concentrations or notches. The tests investigated include the conventional Charpy V-notch, an unnotched bending impact test and an unnotched tension impact test. These tests vary with respect to the strain rate, the presence of a notch, the stress distribution and the amount of metal that is fractured. The strain rate of the Charpy V-notch impact test is approximately 650 inches per inch per second compared to 220 for the un-

notched bending impact test and only 45 for the bending impact test. The cross sectional area of the steel fractured is 0.124 sq. in. for the Charpy V-notch, 0.10 sq. in. for the tension impact test and 0.50 sq. in. for the unnotched bend test. Both the Charpy V-notch and the unnotched bending impact provide bending stresses from a simple beam or three point loading arrangement; the tension impact test provides uniaxial tension within the gage length.

Two primary factors are considered in evaluating the results of the impact tests on the sound metal and determining the influence of the various discontinuities. The first is the temperature of the transition of the fracture from ductile to brittle as measured by several methods. This temperature is influenced by the type of test, but for a given test, the lower the temperature of transition, the greater the impact resistance of the steel specimen. Secondly, the energy required to fracture the impact test specimen also has considerable significance, particularly the fracture energy level in the ductile fracture region.

The higher the energy for a cast steel test specimen, the greater the resistance of the steel specimen to failure under impact load. An engineering evaluation of the influence of various metallurgical factors and types of discontinuities is based on the effect of the discontinuity on the transition temperature and fracture energy, tempered by the different conditions involved in each test. It is evident that the higher strain rate and presence of the notch in the Charpy V-notch test produces a higher transition temperature for the same steel. In addition, the energy required to fracture test specimens is generally greatest for the large cross section of the unnotched bending impact test, intermediate for the tension test because of the intermediate volume of metal stressed equally and smallest for the Charpy V-notched test which is fractured with a bending stress.

The results obtained with the impact tests on sound cast steel serve to substantiate the influence of metallurgical factors that have been well established. The improved toughness obtained with a tempered martensitic structure compared to a ferrite-pearlite structure is evident in all three tests. This condition is primarily indicated by the lower transition temperature of the steels with the tempered martensitic structure. The advantages of the liquid quenching and tempering treatments over normalizing and tempering cycles is thereby illustrated.

The research of this investigation shows that the levels of ductile fracture energy tend to be higher in some cases for the normalized and tempered steels than for the quenched and tempered because of the higher strength level obtained with the quenching and tempering treatment. However, it is generally established that the level of ductile fracture energy decreases with increasing strengths. When the tempering temperatures are adjusted to produce the same strength level, the fracture energy of the quenched and tempered cast steel specimens for all tests are always higher.

A severe loss in toughness resulted from the presence of discontinuities on cast steel surfaces. This lower toughness occurred for all tests and at both strength levels. It should be remembered in evaluating these studies that the discontinuities were all greater than those permitted by the ASTM reference radiographs of E71 and E99 even for the most severe class. The preparation of discontinuities in small test specimens is a most difficult undertaking and hence the discontinuities are gross in character. It is practically impossible to prepare specimens with gradations in severity similar to those shown in the ASTM reference radiographs. This does not mean that discontinuities of less severity than those studied in this research would show higher impact energies but it does illustrate what is possible under most severe conditions. Also the test section is reduced because of the presence of the discontinuities and this condition itself results in a reduction in the impact energy. This change in dimensions may also change the transition temperature.

Surface discontinuities as compared to internal discontinuities are more severe in lowering impact energy of bending specimens not only because of stress concentration at the surface discontinuity but also because of the severity of the notch resulting from the nature of the discontinuity. Hot tears which exist at the surface of cast steel and extend inward are responsible for a severe loss in impact energy. Considerable scatter was present depending on the location and severity of the hot tears but the over-all results are conclusive. The presence of hot tears of the considerable severity tested in this investigation is unacceptable in steel castings that are to be utilized in impact applications. This is in accordance with the present ASTM nondestructive tests reference standards.

The presence of severe gas cavities on the surface of cast steel also produced a considerable increase in transition temperature and a decrease in the level of fibrous impact energy for both the unnotched bend and tensile impact tests on cast steel. This loss occurred with both heat treatments and strength levels. It is indicated that the presence of severe gas cavities in the highly stressed areas subject to impact loading would render steel castings unsuitable for moderate to critically stressed impact service.

The increase in transition temperature and decrease in the fibrous level of ductile fracture energy that occurs with severe slag inclusions on the surface of cast steel impact specimens was somewhat less than experienced with hot tears and gas cavities. It was evident, however, that an appreciable loss in impact resistance could result depending upon the location and severity of the discontinuity. The utilization of steel castings with surface slag inclusions in critically stressed areas for impact service does not appear advisable but the casting may well be suitable for uses involving mild impact loads.

Comparison of the impact test data obtained with the sound cast and sound welded cast steel permits an evaluation of the effect of welding on impact resistance. It is necessary to allow for the variations in strength level that resulted in some of the specimens because of the difficulty in matching the exact heat treatment response of the cast steel with weld deposit in order to obtain a comparable strength. The impact resistance of sound cast steel was similar to the sound machined welded cast steel.

The presence of the complete weld deposit in the sound as-welded but not machined welded specimen reduces the impact resistance to some degree compared to the welded machined specimen. This loss in impact resistance is not large but occurs consistently and is particularly evident in decreasing the level of ductile fracture energy. It apparently results from the stress concentration at the junction of the raised weld deposit and the smooth contour of the specimen. These results indicate the necessity of matching the heat treatment response of the weld deposit with the casting as closely as possible to obtain equivalent strength and machining the weld deposit to follow the uniform contour of the part for good impact resistance.

The influence of severe welding discontinuities varies to some extent depending upon the type of impact test. The loss in impact resistance, as

measured by both the transition temperature and level of ductile impact resistance, is less for incomplete penetration than for undercuts or slag inclusions with both tests. However, the decrease in impact resistance from incomplete penetration is significant for both bending and tension impact, indicating the undesirability of utilizing welded steel with this discontinuity for the more severe impact applications. Severe undercut discontinuities produce the most serious loss in impact resistance, as measured by both criteria, when the bending stresses occur, since this is a surface discontinuity. Severe slag inclusions result in the greatest loss of toughness under tension impact stresses since this stressing is uniform across the gage section and slag inclusions are more randomly oriented. For similar reasons, the undercut discontinuity results in intermediate damage to the impact resistance in the tension test and slag produces an intermediate loss in toughness with the unnotched bead specimens.

From an engineering standpoint, any discontinuity in a cast steel section subject to dynamic loading in impact will reduce the impact resistance of the section. Whether the section and the composite structure, the steel casting, is acceptable for a given application that involves suddenly applied loads depends upon the magnitude of the load, detailed dimensions of the highly stressed area, rate of application of load and the temperature of service. Hot tears render a stressed section unsuitable for any type of impact service; severe gas cavities also restrict the use of sections for all but the mildest type of impact use. Slag inclusions and undercuts in welds in cast steel reduce the toughness of welded cast steel considerably; the undercuts are more damaging under bending and the slag reduces toughness to a greater extent in tension. Incomplete penetration only lowers the toughness of welded cast steel to a slight extent. The presence of slag or undercuts in welds severely restricts their use in impact while lack of complete penetration can be permitted except in severe applications.

Conclusions

1. The tempered martensitic structure produced by quenching and tempering the low alloy cast steel (8630) provided better impact resistance than the ferritic-pearlitic structure obtained by quenching and tempering. This improvement in toughness was particularly marked in its effect on the transition temperatures obtained with the three types of impact tests. The levels of ductile fracture energy tended to be somewhat higher in

some cases for the normalized and tempered cast steels because of the higher strength (130,000 to 150,000 psi) of the quenched and tempered compared to the normalized and tempered cast steels (80,000 to 90,000 psi). When the tempering temperatures are adjusted to produce the same strength level (110,000 to 120,000 psi), the fracture energy of the quenched and tempered cast steel for all tests is always higher.

2. Severe discontinuities present at the surface of cast steels result in increased transition temperatures and diminished fracture energies as compared to sound cast steel. Impact ductility and fracture energy in bending are dependent on both the location of the discontinuity and the stress concentration produced by the discontinuity. The location does not appear to be a major factor in the tension impact test because of the larger volume of metal stressed equally. The loss of impact properties in bending impact and tension impact was dependent on the severity of surface discontinuities. Hot tears produced the greatest loss in toughness followed by severe gas cavities and surface slag inclusions in that order. In all cases, the discontinuities tested were more severe than those specified in ASTM non-destructive testing reference standards. The results do not permit any conclusions concerning the influence of other than severe discontinuities on impact behavior.

3. The toughness of welded cast steel with the weld machined to the contour of the specimen surface was similar to cast steels processed to the same strength levels by a similar heat treatment. The sound, as-welded cast steel specimens with the weld deposit in place exhibited a loss in toughness as indicated by reduced fracture energies because of the mild notch effect at the edge of the reinforcing bead at the surface. The other weld discontinuities reduced the impact resistance to a greater extent. The order of decreasing severity when testing in bending impact was undercut, surface slag, slag inclusion located midway near the specimen surface and incomplete penetration, located internally. Testing by tension impact showed that slag inclusions were the most detrimental followed by undercut and incomplete penetration. Again the weld discontinuities were gross and judged to be of greater severity than illustrated by the ASTM non-destructive testing reference standards. No conclusions can be made concerning the effect of discontinuities of less severity.

4. Brittle fracture energies measured near the ductility transition temperature by bending impact and tension impact for casting discontinuities appear to be related to the stress concentration of the discontinuity (proportional to K_t^{-2}). The higher stress concentrations produced by hot tear discontinuities are more damaging to the impact properties than that produced by the severe gas cavities and slag discontinuities. The K_t values estimated for the slag and gas cavity discontinuities for both tensions and bending were within the range of 1.5 to 2.6. The stress concentration values produced by hot tears are 9 and greater.

5. From an engineering standpoint, the following evaluations of the effect of severe discontinuities on impact service of steel castings is made.

- a. Surface hot tears make the casting unacceptable.
- b. Severe gas cavities at casting surfaces and undercuts and slag inclusions in welded cast steel restrict the use of steel castings for impact service.
- c. Castings with severe slag inclusions and lack of penetration in welds should be serviceable for milder impact application.

REFERENCES

1. Acker, H. G., "Review of Welded Ship Failures," Welding Research Council No. 19, November 1954.
2. Shank, M. E., "Brittle Fracture in Carbon Plate Steel Structures Other than Ships," Welding Research Council No. 17, January 1954.
3. Shank, M. E., ed., "Control of Steel Construction to Avoid Brittle Fracture," American Welding Society, 1957.
4. Clark, D. S., ASM Transactions, Vol. 46, 1954, p. 34.
5. Dieter, G. E., "Mechanical Metallurgy," McGraw-Hill, 1961.
6. Offenshausen, C. M., and Koopman, K. N., "Factors Effecting the Weldability of Carbon and Alloy Steels," Welding Journal Research Supplement, May 1948, pp. 2345-2525.
7. Wood, D. S., and Clark D. S., ASM Transactions, Vol. 43, 1951, p. 571.
8. Holloman, J. H., "The Notched Bar Impact Test," AIME Transactions, Vol. 58, 1944, pp. 298-327.
9. Boodberg, H., et al., "Causes of Cleavage Fracture in Ship Plate Tests of Wide Notched Plates," The Welding Journal Research Supplement 27, 1948, p. 186.
10. Wilson, W. M., et al., "Cleavage Fracture of Ship Plates as Influenced by Size Effect," The Welding Journal Research Supplement 27, 1948, 200-5.
11. Stout, R. D., "Engineering Aspects of Evaluating Notch Toughness," Fracture of Engineering Materials, ASM, 1959, p. 19.
12. McNicol, R. C., "Correlation of Charpy Test Results for Standard and Non-Standard Size Specimens," Welding Research Supplement, September 1965, 385S.
13. Fearnough, G. D., "Influence of Specimen Size in a Drop Weight Test on Large Vee Notched Bend Specimens," British Welding Journal, December 1963, Vol. 10, No. 12, 607.
14. Holloman, J. H., et al., "The Effects of Microstructure on the Mechanical Properties of Steel," Transactions ASM, Vol. 38, 1947.
15. Gillet, H. W., and McGuire, F. T., "Report on Behavior of Ferritic Steels at Low Temperatures," ASM Publication, 1945.
16. Rosenthal, P. C., and Manning, G. K., "Heat Treatment of Heavy Cast Steel Sections," Foundry, Vol. 74, 1946.
17. Kottcamp, E. H., Jr., and Stout, R. D., "Effect of Microstructure on Notch Toughness, Part IV," October 1959.
18. Gross, J. H., and Stout, R. D., "Effect of Microstructure on Notch Toughness, Part III," Welding Journal 35, No. 2, 725, 1956.
19. Gensamer, M., "Brittle Fracture of Metals," Fracture of Engineering Materials, ASM, August 1959.
20. Rinebolt, J. A., and Harris, W. J., Jr., "Effect of Alloying Elements on the Notch Toughness of Pearlitic Steels," ASM Transactions, Vol. 43, 1951, pp. 1175-1204.
21. Szczpanski, M., "The Brittleness of Steel," John Wiley & Sons, 1963.
22. Parker, E. R., "Brittle Behavior of Engineering Structures," John Wiley & Sons, Inc., 1957, p. 397.
23. Ahearn, P. J., Form, G. W., and Wallace, J. F., "High Strength Steel Castings Mass Effect on Tensile Properties," AFS Trans., Vol. 70, 1962, pp. 1154-1160.
24. Wallace, J. F., Savage, J. H., and Taylor, H. F., "Mechanical Properties of Cast Steel as Influenced by Mass and Segregation," AFS Trans., Vol. 59, 1951, pp. 223-242.
25. Bramfitt, B. L., and Luizzi, L., "A Study of the Effect of Solidification Imperfections on the Tensile Properties of Cast Steel," Report No. WVT 6420, Watervliet Arsenal, Watervliet, New York, September 1964.
26. Mattek, L. J., and Woodward, R. D., "Correlation of Tensile Properties of Steel Castings and Material Imperfections as Determined by Radiography," WAD Technical Report 60-450, February 1961.
27. Mattek, L. J., "Correlation of Radiographically Observed Flaws with Tensile Properties of Stainless Steel Castings," Materials Research & Standards, Vol. 2, No. 8, August 1962, p. 633.
28. Turnbull, G. K., and Wallace, J. F., "Effect of Shrinkage Porosity on Mechanical Properties of Steel Casting Sections," Steel Foundry Research Foundation, Cleveland, Ohio, January 1962.
29. Green, W. F., Hammad, M. F., and McCauley, R. B., "The Effect of Porosity on Mild Steel Welds," The Welding Research Supplement, 37 (7), 1958, pp. 2065-2095.
30. Bradley, J. W., and McCauley, R. B., "The Effect of Porosity in Quenched and Tempered Steel," Welding Research Supplement, September 1964, pp. 4085-4145.
31. Vishnesky, C., Bertolino, N. F., and Wallace, J. F., "The Effects of Surface Discontinuities on the Fatigue Properties of Cast Steel Sections," Steel Foundry Research Foundation, Rocky River, Ohio, August 1966.
32. Steigerwald, E. A., "Influence of Decarburization on the Notch Sensitivity of High Strength Steel," TM 1547 CM, TRW Inc., Cleveland, Ohio, February 23, 1960.
33. Bridgeman, P. W., "Studies in Large Plastic Flow and Fracture," Harvard University Press, Cambridge, Mass., 1964.
34. Mann, H. C., "Relation of Impact and Tension Tests of Steel," Metal Progress, March 1935.
35. Felback, D. K., and Orowan, E., "Experiments on the Brittle Fracture of Steel Plates," The Welding Research Supplement, pp. 5705-5755, 1955.
36. Lipson, C., and Juvinall, R. C., Handbook of Stress and Strength, McMillan Co., New York, 1963.
37. Peterson, R. E., Stress Concentration Design Factors, John Wiley & Son, Inc., New York, 1953.
38. Neuber, H., Theory of Notch Stresses, Edwards Brothel's, Inc., 1946.

APPENDIX I

TABLE 8

Charpy "V" Notch Impact Test Results

Temperature (°F)	Lateral Expansion (%)	Energy (Ft.-Lbs.)	Percent Fibrous
Heat B—Quench & Temper 149,000 psi - U.T.S.			
Composition: C .33, Mn .89, Si .38, Cr .45, Ni .55, Mo .25, P .027, S .030, Al .032			
-321	0	5.0	0
-200	0.76	10.0	10
-150	0.76	11.5	40
-100	2.54	14.0	40
-50	3.04	24.0	50
0	3.81	22.0	60
+75	5.33	29.5	100
+350	5.83	28.0	100
Heat C—Normalize & Temper 93,800 psi - U.T.S.			
Composition: C .31, Mn .64, Si .26, Cr .45, Ni .55, Mo .25, P .026, S .029, Al .070			
-321	0	1.0	0
-100	0.51	3.0	0
0	0.51	4.5	0
+75	3.30	12.5	50
+125	6.34	17.5	60
+200	8.38	25.0	80
+250	10.41	29.0	100
+350	15.74	28.5	100
Heat G—Quench & Temper 141,300 psi - U.T.S.			
Composition: C .32, Mn .84, Si .37, Cr .60, Ni .60, Mo .19, P .030, S .032			
-321	0	3.5	0
-200	0.25	5.0	0
-150	1.27	8.0	10
-125	1.52	9.0	20
-100	1.78	11.0	25
-75	3.04	16.5	30
-50	3.56	19.0	50
0	3.81	20.0	80
+32	3.81	28.0	100
+75	5.33	28.5	100
+250	5.83	25.5	100
+430	5.83	26.0	100
Heat H—Normalize & Temper 91,100 psi - U.T.S.			
Composition: C .32, Mn .80, Si .52, Cr .45, Ni .60, Mo .21, P .027, S .028			
-321	0	1.0	0
-200	0	1.0	0
-100	0.51	2.0	0
-50	1.27	4.5	10
0	2.03	7.0	20
+32	2.03	8.5	20
+75	4.83	15.5	50
+125	6.34	21.5	70
+200	9.14	30.0	100
+250	10.41	33.5	100
+350	10.41	33.5	100
+490	10.41	31.5	100

TABLE 8—(Continued)

Temperature (°F)	Lateral Expansion (%)	Energy (Ft.-Lbs.)	Percent Fibrous
Heat D-1—Quench & Temper 111,000 psi - U.T.S.			
Composition: C .30, Mn .73, Si .40, Cr .40, Ni .63, Mo .20, P .014, S .013, Al .050			
-321	0	2.0	0
-200	0.51	2.5	0
-200	1.52	6.5	10
-150	2.79	14.0	20
-125	3.81	17.0	40
-100	4.83	25.0	70
-50	7.36	34.5	90
0	7.36	39.0	90
+75	9.64	44.5	100
+200	10.17	45.5	100
+350	12.21	43.5	100
+450	12.97	42.0	100
Heat D-2—Normalize & Temper 119,200 psi - U.T.S.			
-321	0	1.5	0
-100	0	4.0	10
0	1.27	7.5	20
+32	1.27	7.0	20
+75	3.30	13.0	30
+100	4.06	16.0	40
+125	4.83	21.5	60
+175	7.36	32.0	90
+200	8.38	35.5	100
+250	7.62	38.5	100
+350	11.68	37.0	100
+450	9.14	35.5	100
Heat O—Quench & Temper 134,100 psi - U.T.S.			
Composition: C .33, Mn .85, Si .30, Cr .45, Ni .55, Mo .25, P .029, S .032, Al .090			
-321	0	4.0	0
-250	0	5.0	0
-200	1.02	9.0	0
-150	7.87	12.5	—
-125	3.30	15.0	40
-50	5.58	25.0	50
0	7.36	32.0	75
+32	7.87	32.0	100
+75	7.62	30.5	100
+350	—	30.5	100
Heat O—Normalize & Temper 90,400 psi - U.T.S.			
-321	0	2.0	0
-200	0	4.5	0
-150	0.76	5.5	10
-100	2.79	5.0	10
0	6.60	5.0	20
+32	7.87	13.0	30
+75	11.68	15.5	50
+75	12.97	13.0	40
+125	12.97	22.0	70
+200	12.97	30.0	100
+250	15.50	33.5	100
+350	15.50	33.0	100

TABLE 9
Unnotched Bending Impact
Test Results for Casting Discontinuities

Temperature (°F)	Energy (Ft.-Lbs.)	Lateral Contraction (%)	Percent Fibrous
Heat A—Quench & Temper 132,000 psi - U.T.S.			
Composition: C .33, Mn .90, Si .28, Cr .45 Ni .55, Mo .25, P .027, S .032, Al .070			
-321	443	0.9	40
-321	164	0.5	30
-250	702	7.7	80
-200	720	8.3	80
-100	875	11.0	100
-40	900	8.5	100
-40	820	10.0	100
+75	1010	13.6	100
+75	836	13.0	100
+200	884	13.1	100
Heat A—Normalize & Temper 88,000 psi - U.T.S.			
-321	41	0	0
-250	117	0.3	0
-200	186	1.0	10
-150	302	4.4	20
-150	328	4.6	25
-125	614	9.8	50
-75	1013	10.0	60
-40	1203	16.4	100
-40	1277	15.8	*100
+35	1277	15.4	*100
+75	1223	16.0	*100
+200	1220	14.2	*100
* Specimen stayed in one piece - bend through on angle of ~112°			
Gas Cavities			
Heat J—Quench & Temper 136,200 psi - U.T.S.			
Composition: C .30, Mn .81, Si .29, Cr .45, Ni .55, Mo .25, P .027, S .032, Al .044			
-321	32	0	0
-200	72	—	10
-150	183	1.0	—
-150	118	1.0	50
-100	104	1.0	70
-40	177	0.9	80
-40	128	1.7	90
+75	202	0.7	100
+75	218	2.0	100
+200	146	0.7	100
+200	146	1.0	100
+200	229	0.8	100
+400	183	—	100
+500	236	1.4	100
+600	185	1.6	100

TABLE 9—(Continued)

Temperature (°F)	Energy (Ft.-Lbs.)	Lateral Contraction (%)	Percent Fibrous
Gas Cavities			
Heat J—Normalize & Temper 82,700 psi - U.T.S.			
-321	32	0	0
-321	32	0	0
-200	28	0	0
-150	41	0	0
-100	243	3.5	20
-100	70	0	10
-100	117	0.8	10
-40	164	0.2	10
-40	117	0.4	10
-40	128	0.8	10
+35	277	2.9	80
+75	338	3.6	100
+200	426	3.8	100
+200	400	5.1	100
+400	293	—	100
+500	450	4.5	100
+600	400	7.0	100
Surface Slag Inclusions			
Heat K—Quench & Temper 131,200 psi - U.T.S.			
Composition: C .31, Mn .85, Si .21, Cr .45, Ni .55, Mo .25, P .028, S .030			
-321	37	0	0
-200	134	0.9	30
-150	216	—	50
-125	250	1.3	70
-100	460	3.7	80
-75	300	3.5	90
-40	385	3.0	100
+35	323	2.4	100
+75	460	4.5	100
+200	393	3.9	100
+400	343	4.3	100
Surface Slag Inclusions			
Heat K—Normalize & Temper 90,300 psi - U.T.S.			
-321	28	0	0
-200	28	0	10
-150	84	0.4	20
-100	80	0.4	20
0	502	5.6	70
+35	511	6.8	70
+75	380	3.0	90
+75	451	5.0	90
+200	590	6.5	100
+400	484	5.8	100

TABLE 9—(Continued)

Temperature (°F)	Energy (Ft.-Lbs.)	Lateral Contraction (%)	Percent Fibrous
Hot Tears			
Heat L—Quench & Temper			
131,600 psi - U. T. S.			
Composition: C .32, Mn .72, Si .19, Cr .45, Ni .55, Mo .25, P .028, S .031, Al .023			
-321	28	0	0
-321	28	0	0
-321	46	0	0
-321	20	0	0
-321	32	0	0
-321	64	0	0
-200	50	0	10
-200	46	0	10
-150	70	0.4	20
-40	70	1.0	60
-40	95	0.8	70
-40	74	0.4	70
-40	106	1.0	70
-40	32	0.2	80
-40	209	1.8	80
-40	79	0.4	80
-40	106	0.8	70
+75	106	2.2	100
+75	146	0.7	100
+75	140	1.6	100
+200	229	0.9	100
+200	123	1.8	100
+200	106	1.5	100
+200	79	1.4	100
+200	209	2.7	100
+200	112	0.8	100
+200	134	1.7	100
+200	177	3.2	100
+200	140	0.6	100
+200	146	2.9	100
+200	128	2.0	100
+300	79	2.0	100
+300	223	2.6	100
+300	123	2.0	100
+300	183	3.0	100
+300	90	1.2	100
+400	74	0.5	100
+400	90	0.5	100
+400	146	2.5	100
+400	323	4.8	100
+400	123	1.0	100
+400	90	2.0	100
+400	79	0.5	100
+400	134	1.5	100
+400	223	3.7	100
+500	47	0.8	100
+500	600	—	100
+500	293	2.2	100
+500	140	1.8	100
+500	434	—	100
+500	146	1.5	100
+600	293	2.7	100
+600	216	2.8	100
+600	209	3.0	100
+600	223	3.5	100

TABLE 9—(Continued)

Temperature (°F)	Energy (Ft.-Lbs.)	Lateral Contraction (%)	Percent Fibrous
Hot Tears			
Heat L—Normalize & Temper			
85,600 psi - U.T.S.			
-321	28	0	0
-321	28	0	0
-321	24	0	0
-321	32	0	0
-321	28	0	0
-321	32	0	0
-200	85	0	0
-200	32	0	0
-200	100	0	0
-200	28	0	0
-40	50	0	10
-40	95	0.5	30
-40	28	0	10
-40	46	0	10
-40	447	—	—
-40	106	0.5	20
-40	40	0	20
-40	80	1.1	30
+75	286	2.8	70
+75	377	3.0	70
+75	582	—	90
+75	502	—	100
+75	164	2.2	70
+200	209	5.5	100
+200	494	—	100
+200	216	3.9	100
+200	293	3.9	100
+210	1074	—	100
+200	146	2.7	100
+200	346	4.4	100
+200	128	0.9	100
+200	331	5.0	100
+200	257	4.0	100
+210	954	—	100
+300	79	1.3	100
+300	370	6.0	100
+300	236	4.3	100
+400	264	3.3	100
+400	362	5.5	100
+400	300	1.2	100
+400	570	—	100
+400	250	4.8	100
+400	70	0.4	100
+500	140	0.7	100
+500	209	4.6	100
+500	271	4.4	100
+500	331	2.5	100
+500	229	5.7	100
+500	278	—	100
+600	208	4.0	100
+600	331	4.5	100
+600	300	4.4	100
+600	370	4.8	100
+600	537	—	100
+600	183	1.9	100

TABLE 10

**Unnotched Tension Impact
Test Results for Casting Discontinuities**

Gas Cavities
Heat B—Quench & Temper
149,300 psi - U.T.S.

Temp. (°F)	Energy (Ft.-Lbs.)	% R. A.	% El.	% Fibrous
-321	30	0	0	0
-250	70	0	0	20
-250	76	1.1	0.56	20
-200	76	4.9	0.56	30
-200	92	3.3	0.56	30
-110	82	—	—	60
-110	96	7.6	1.12	80
-50	—	8.7	0.56	90
0	92	7.6	1.12	100
+75	96	11.4	1.69	100
+75	86	10.3	1.69	100
+200	108	11.9	1.12	100
+400	110	11.9	1.69	100

Gas Cavities
Heat C—Normalize & Temper
93,800 psi - U.T.S.

Temp. (°F)	Energy (Ft.-Lbs.)	% R. A.	% El.	% Fibrous
-321	16	0	—	0
-250	52	0	0	0
-200	48	0	0	0
-200	44	0	0	0
-150	72	7.1	0.56	10
-110	104	8.7	0.56	40
-110	—	7.6	0.56	40
-110	72	8.7	0.56	40
0	118	5.5	0.56	60
+75	110	23.1	4.49	100
+200	132	25.1	5.06	100
+400	116	29.4	5.06	100

Slag Inclusions
Heat M—Quench & Temper
136,500 psi - U.T.S.
Composition: C .28, Mn .78, Si .20, Cr .45, Ni .55, Mo .25,
P .028, S .030

Temp. (°F)	Energy (Ft.-Lbs.)	% R. A.	% El.	% Fibrous
-321	58	0	0	10
-321	36	0	0	10
-250	104	2.7	0.56	20
-250	70	2.7	0.56	20
-200	80	1.1	0.56	30
-200	80	—	—	30
-110	80	4.9	1.69	70
-110	100	4.4	—	70
0	130	9.3	—	100
+75	100	9.3	2.25	100
+75	124	9.3	2.81	100
+200	110	2.7	1.12	100
+350	148	4.5	5.62	100
+400	136	1.4	4.49	100

TABLE 10—(Continued)

Slag Inclusions
Heat M—Normalize & Temper
84,400 psi - U.T.S.

Temp. (°F)	Energy (Ft.-Lbs.)	% R. A.	% El.	% Fibrous
-321	16	0	0	0
-250	50	0	0	0
-250	44	0	0	10
-200	40	2.2	0.56	20
-200	45	1.1	0.56	20
-110	64	2.7	0.56	30
-110	76	2.7	0.56	30
-50	140	—	—	50
+75	160	8.7	3.93	100
+75	150	21.9	4.81	100
+100	150	22.5	6.74	100
+150	173	27.0	15.17	100
+200	164	24.5	11.79	100
+200	175	19.6	11.79	100
+400	168	21.1	11.79	100

Hot Tears
Heat N—Quench & Temper
129,200 psi - U.T.S.
Composition: C .31, Mn .66, Si .23, Cr .45, Ni .55, Mo .25,
P .027, S .030

Temp. (°F)	Energy (Ft.-Lbs.)	% R. A.	% El.	% Fibrous
-321	72	0	0	0
-321	12	0	0	0
-250	50	0	0	0
-200	32	0	0	10
-200	50	—	—	20
-110	78	1.1	1.12	50
-110	68	1.1	1.12	80
0	95	—	—	—
+75	66	—	—	100
+75	84	7.6	1.69	100
+200	72	9.3	2.81	100
+400	92	13.5	5.62	100

Hot Tears
Heat N—Normalize & Temper
90,500 psi - U.T.S.

Temp. (°F)	Energy (Ft.-Lbs.)	% R. A.	% El.	% Fibrous
-321	32	0	0	0
-200	42	0	0	0
-200	20	0	—	10
-110	25	0.5	0.56	10
0	68	2.7	0.56	50
+75	50	—	—	60
+150	—	10.6	1.35	75
+200	110	22.1	3.55	100
+400	100	17.6	—	100

* Specimen stayed in one piece - bend angle ~112°

TABLE 11

**Unnotched Bending Impact
Test Results For Weld Discontinuities**

Welded Sound, Machined
Heat O—Quench & Temper
134,100 psi - U.T.S.

Temp. (°F)	Energy (Ft.-Lbs.)	Lateral Contraction (%)	Percent Fibrous
-321	79	0	10
-250	1013	15.7	80
-200	1221	15.4	90
-150	1533	23.7	*100
-150	1320	13.2	100
-125	1533	25.0	*100
-100	1515	23.6	*100
-40	1469	23.2	*100
-40	1412	24.4	*100
+35	1460	24.5	*100
+75	1375	25.5	*100
+200	1378	25.5	*100

Welded Sound, Machined
Heat O—Normalize & Temper
90,400 psi - U.T.S.

Temp. (°F)	Energy (Ft.-Lbs.)	Lateral Contraction (%)	Percent Fibrous
-321	37	0	0
-250	70	0	0
-200	106	0.4	10
-150	920	22.1	80
-150	364	0.6	10
-100	1341	22.8	*100
-100	1300	14.7	90
-40	1302	17.5	*100
-40	1302	17.2	*100
+75	1350	16.8	*100
+75	1182	15.5	*100
+200	1262	21.3	*100

Welded Sound, As Welded
Heat O—Quench & Temper
134,100 psi - U.T.S.

Temp. (°F)	Energy (Ft.-Lbs.)	Lateral Contraction (%)	Percent Fibrous
-321	55	0	20
-250	1013	0.3	70
-200	951	6.4	80
-150	944	3.5	*100
-100	1112	4.4	*100
-75	930	6.4	90
-40	1200	15.0	*100
-40	1100	10.0	*100
+35	944	11.8	*100
+75	1223	16.2	*100
+75	1140	15.9	*100
+200	1208	16.0	*100

TABLE 11—(Continued)

Welded Sound, As Welded
Heat O—Normalize & Temper
90,400 psi - U.T.S.

Temp. (°F)	Energy (Ft.-Lbs.)	Lateral Contraction (%)	Percent Fibrous
-321	55	0	0
-250	70	0	0
-200	383	7.1	30
-200	55	0	0
-150	383	6.4	30
-125	934	10.8	80
-100	875	10.0	80
-100	1201	8.8	90
-40	1280	13.5	*100
+35	1201	11.3	*100
+75	1301	14.1	*100
+75	1250	15.0	*100
+200	1213	11.5	*100

Welded, Slag Porosity
Heat O—Quench & Temper
134,100 psi - U.T.S.

Temp. (°F)	Energy (Ft.-Lbs.)	Lateral Contraction (%)	Percent Fibrous
-321	37	0	10
-200	74	0.8	20
-150	117	1.1	40
-100	583	9.3	80
-100	308	5.1	40
-40	564	8.4	100
-40	537	9.5	100
+75	590	9.2	100
+75	480	8.0	100
+200	531	9.9	100
+400	557	7.7	100

Welded, Incomplete Penetration
Heat O—Normalize & Temper
90,400 psi - U.T.S.

Temp. (°F)	Energy (Ft.-Lbs.)	Lateral Contraction (%)	Percent Fibrous
-321	55	0	0
-321	41	0	0
-200	41	0	10
-150	520	5.8	20
-125	365	11.5	0
-100	655	11.7	80
-40	788	15.8	100
-40	944	13.5	*100
+75	792	13.2	*100
+200	875	14.3	*100
+400	794	17.3	*100

* Specimen stayed in one piece - bend angle ~112°

TABLE 11—(Continued)

Welded, Undercut
Heat O—Quench & Temper
134,100 psi - U.T.S.

Temp. (°F)	Energy (Ft.-Lbs.)	Lateral Contraction (%)	Percent Fibrous
-321	46	0	0
-321	28	0	0
-200	28	0	10
-200	140	0.8	30
-150	152	0.8	40
-100	354	4.1	90
-40	546	8.3	100
-40	477	5.1	90
+75	511	6.5	100
+200	477	5.0	100
+400	520	7.8	100

Welded, Undercut
Heat O—Normalize & Temper
90,400 psi - U.T.S.

Temp. (°F)	Energy (Ft.-Lbs.)	Lateral Contraction (%)	Percent Fibrous
-321	32	0	0
-321	24	0	0
-200	46	0	10
-150	46	0	0
-125	346	4.5	30
-100	338	4.2	30
-40	264	3.0	30
-40	573	5.3	70
+75	537	—	100
+200	628	11.2	*100
+400	434	5.7	100

* Specimen stayed in one piece - bend angle ~112°

TABLE 11—(Continued)

Welded, Incomplete Penetration
Heat O—Quench & Temper
134,100 psi - U.T.S.

Temp. (°F)	Energy (Ft.-Lbs.)	Lateral Contraction (%)	Percent Fibrous
-321	55	0	0
-250	95	0.8	10
-200	308	1.7	70
-150	610	6.1	90
-100	632	7.3	90
-40	494	10.3	90
-40	637	—	100
+75	650	12.2	*100
+75	766	14.0	*100
+200	628	9.8	100
+200	655	9.4	*100
+400	665	10.3	*100

Welded, Slag Porosity
Heat O—Normalize & Temper
90,400 psi - U.T.S.

Temp. (°F)	Energy (Ft.-Lbs.)	Lateral Contraction (%)	Percent Fibrous
-321	41	0	0
-200	85	0.6	10
-125	434	6.9	20
-100	402	5.3	20
-40	637	8.1	80
-40	426	6.2	70
+75	730	2.4	*100
+200	750	9.8	*100
+200	933	5.5	*100
+400	734	5.1	*100

* Specimen stayed in one piece - bend angle ~112°

TABLE 12

**Unnotched Tension Impact
Test Results for Weld Discontinuities**

Welded Sound, Machined
Heat B—Quench & Temper
149,800 psi - U.T.S.

Temp. (°F)	Energy (Ft.-Lbs.)	% R. A.	% El.	% Fibrous
-321	48	0	0	20
-250	80	1.1	0.56	50
-250	86	1.1	0.56	50
-200	235	3.8	1.69	50
-200	305	3.3	1.69	60
-150	309	45.7	8.43	100
-110	295	52.9	—	100
-110	282	53.3	8.43	100
0	323	54.1	8.99	100
+75	383	59.9	11.23	100
+200	277	59.9	11.79	100
+400	292	58.9	10.10	100

Welded Sound, Machined
Heat C—Normalize & Temper
93,800 psi - U.T.S.

Temp. (°F)	Energy (Ft.-Lbs.)	% R. A.	% El.	% Fibrous
-321	62	0	0	10
-250	48	—	—	10
-200	126	2.0	1.10	50
-200	188	—	—	80
-110	345	41.5	14.60	100
-110	387	47.0	—	100
+75	393	64.4	17.98	100
+75	347	63.7	17.98	100
+75	327	61.0	16.85	100
+200	343	67.4	16.29	100
+200	312	63.7	17.42	100
+400	320	66.7	17.42	100

Welded Sound, As Welded
Heat C—Normalize & Temper
93,800 psi - U.T.S.

Temp. (°F)	Energy (Ft.-Lbs.)	% R. A.	% El.	% Fibrous
-321	0	0	0	0
-250	40	0	—	10
-200	60	1.2	—	30
-200	118	2.1	—	30
-150	150	38.9	5.62	60
-110	259	43.6	7.30	90
-50	305	—	—	100
+75	—	45.3	12.92	100
+75	—	41.9	14.02	100
+75	279	45.3	12.92	100
+200	295	44.1	10.10	100
+400	272	47.0	12.92	100

TABLE 12—(Continued)

Welded Sound, As Welded
Heat B—Quench & Temper
149,300 psi - U.T.S.

Temp. (°F)	Energy (Ft.-Lbs.)	% R. A.	% El.	% Fibrous
-321	8	0	0	10
-250	—	1.1	—	40
-200	225	3.8	1.69	80
-110	251	32.2	9.30	100
0	311	—	—	100
+75	261	38.5	11.23	100
+200	283	31.7	9.30	100
+400	266	31.7	1.10	100

Welded, Undercut
Heat B—Quench & Temper
149,300 psi - U.T.S.

Temp. (°F)	Energy (Ft.-Lbs.)	% R. A.	% El.	% Fibrous
-321	38	0	0	0
-321	38	0	0	0
-200	70	0	0	10
-200	96	1.1	0.56	10
-150	196	18.2	4.06	90
-110	204	11.6	4.06	90
-110	196	—	—	—
-110	—	20.4	—	100
-110	—	26.1	5.52	90
0	222	29.4	6.74	100
+75	196	31.7	6.18	100
+200	184	26.5	5.62	100
+400	206	26.0	5.62	100

Welded, Undercut
Heat C—Normalize & Temper
93,800 psi - U.T.S.

Temp. (°F)	Energy (Ft.-Lbs.)	% R. A.	% El.	% Fibrous
-321	16	0	0	0
-250	58	0	0	10
-200	76	0	0	10
-200	68	0	0	10
-150	94	0.5	0.56	20
-150	44	0.5	0.56	20
-110	222	0.5	1.12	60
-110	200	51.0	14.02	90
-110	162	47.0	13.48	100
-50	256	41.1	12.92	100
+75	232	43.6	12.92	100
+200	212	40.7	10.10	100
+400	236	47.0	13.48	100

TABLE 12—(Continued)

Welded, Slag Porosity
Heat B—Quench & Temper
149,300 psi - U.T.S.

Temp. (°F)	Energy (Ft.-Lbs.)	% R. A.	% El.	% Fibrous
-321	16	0	0	0
-250	40	0	0	10
-200	20	0	0	10
-200	0	0	0	10
-150	38	0	0.56	20
-110	56	4.1	1.52	40
-110	86	5.6	1.72	60
0	114	13.5	2.25	100
+75	76	18.6	2.81	100
+75	100	18.6	2.81	100
+200	80	19.1	2.81	100
+400	86	20.6	2.81	100

Welded, Slag Porosity
Heat C—Normalize & Temper
93,800 psi - U.T.S.

Temp. (°F)	Energy (Ft.-Lbs.)	% R. A.	% El.	% Fibrous
-321	18	0	0	0
-250	18	0	0	0
-250	—	0	0	0
-200	44	0	0	0
-200	54	0	0	10
-110	32	3.8	0.56	20
-110	58	6.0	1.69	20
-50	60	2.2	1.12	25
0	110	12.6	4.49	80
0	140	23.1	5.43	90
+75	146	24.6	7.30	100
+200	166	22.1	6.74	100
+400	178	25.5	7.86	100

TABLE 12—(Continued)

Welded, Incomplete Penetration
Heat B—Quench & Temper
149,300 psi - U.T.S.

Temp. (°F)	Energy (Ft.-Lbs.)	% R. A.	% El.	% Fibrous
-321	30	0	0	0
-250	18	0	0	0
-250	38	0	0	0
-200	66	1.1	—	20
-200	32	0	0	10
-150	214	20.1	9.70	90
-110	192	20.7	11.79	100
-110	232	25.5	11.79	100
+75	214	24.6	12.92	100
+200	234	34.0	12.36	100
+350	252	35.4	12.92	100
+400	232	40.7	13.48	100

Welded, Incomplete Penetration
Heat C—Normalize & Temper
93,800 psi - U.T.S.

Temp. (°F)	Energy (Ft.-Lbs.)	% R. A.	% El.	% Fibrous
-321	54	0	0	0
-321	62	0	0	0
-200	20	0	0	0
-200	18	0	0	0
-150	50	0.5	0.56	10
-110	218	20.1	—	90
-110	244	22.1	9.70	90
-50	240	27.6	11.79	90
0	270	38.5	11.79	90
+75	258	47.0	12.92	100
+75	244	42.8	12.36	100
+200	250	35.4	12.92	100
+400	230	42.1	13.48	100

This page left blank intentionally.

STEEL FOUNDRY RESEARCH FOUNDATION
Published Research Reports*

Recommended Practice for Repair Welding and Fabrication Welding of Steel Castings, 58 pages	\$.50
Studies of the Design of Steel Castings and Steel Weldments as Related to Methods of their Manufacture, 47 pages	\$.35
Effect of Shrinkage Porosity on Mechanical Properties of Steel Casting Sections, 16 pages	\$.40
Correlation of Destructive Testing of Steel Castings with Stress Analysis and Mechanical Properties	
Part I-A Summary Report, 20 pages	\$.50
Part II-The Detailed Report, 50 pages	\$2.50
The Effect of Surface Discontinuities on the Fatigue Properties of Cast Steel Sections, 28 pages	\$.50
The Evaluation of Discontinuities in Commercial Steel Castings by Dynamic Loading to Failure in Fatigue, 44 pages.....	\$.50
Fatigue of Cast Steels. Part I-A Study of the Notched Effect and of the Specimen Design and Loading. Part II-Fractographic Studies, 28 pages	\$.50
Impact Properties of Cast Steel Sections with Surface Discontinuities	\$.50

* Available to the public at the price shown-Minimum billing \$1.00

STEEL FOUNDRY RESEARCH FOUNDATION

21010 Center Ridge Road Rocky River, Ohio 44116